



The Kostin Equation, the Deceleration of a Quantum Particle and Coherent Control

Harald Losert¹ · Freyja Ullinger^{1,2} · Matthias Zimmermann² · Maxim A. Efremov^{1,2} · Ernst M. Rasel³ · Wolfgang P. Schleich^{1,4}

Received: 25 May 2022 / Accepted: 19 August 2022 / Published online: 19 September 2022
© The Author(s) 2022

Abstract

Fifty years ago Kostin (J Chem Phys 57(9):3589–3591, 1972. <https://doi.org/10.1063/1.1678812>) proposed a description of damping in quantum mechanics based on a *nonlinear* Schrödinger equation with the potential being governed by the phase of the wave function. We show for the example of a moving Gaussian wave packet, that the deceleration predicted by this equation is the result of the same non-dissipative, homogeneous but time-dependent force, that also stops a classical particle. Moreover, we demonstrate that the Kostin equation is a special case of the *linear* Schrödinger equation with three potentials: (i) a linear potential corresponding to this stopping force, (ii) an appropriately time-dependent parabolic potential governed by a specific time dependence of the width of the Gaussian wave packet and (iii) a specific time-dependent off-set. The freedom of the width opens up the possibility of engineering the final state by the time dependence of the quadratic potential. In this way the Kostin equation is a precursor of the modern field of coherent control. Motivated by these insights, we analyze in position and in phase space the deceleration of a Gaussian wave packet due to potentials in the *linear* Schrödinger equation similar to those in the Kostin equation.

Keywords Cooling · Quantum dynamics · Coherent control · Nonlinear Schrödinger equation · Kostin equation · Wigner phase space · Gaussian wave packet

It is with great pleasure that we dedicate this article to David Lee and John Reppy—true pioneers of low temperature physics and wonderful human beings—on the occasion of their 90th birthday. We hope that the topic for our contribution—the deceleration of a quantum particle by time-dependent forces—will find their interest. Two of us (HL and WPS) had the great fortune to have collaborated with David on a nonlinear Schrödinger equation, that is the Leggett equation. For this reason, we are confident that the present study motivated by another nonlinear Schrödinger equation, that is the Kostin equation, might also trigger his curiosity. Moreover, central to our present consideration is the physics of cold atoms. One of us (WPS) remembers fondly discussions with John about the transmission of atoms through porous media during John’s visit to Austin, Texas, in the fall of 1985. These conversations were later instrumental to our thoughts about possible realizations of the quantum version of the Ulm sparrow. Many thanks to both of you for being in our lives and many more happy and healthy years filled with fun of doing science!

Extended author information available on the last page of the article

1 Introduction

Damping in quantum mechanics [1, 2] is a subtle business [3] due to the canonical commutation relations. For this reason, the description of a damped quantum state employs the density operator rather than a wave function. Notwithstanding the fact that the method of quantum trajectories [4] has been rather successful, in particular in the context of laser cooling [5], it seems to be conventional wisdom that a description of damping based on a *single* wave function is impossible.

However, exactly 50 years ago Morton Daniel Kostin proposed [6] a nonlinear Schrödinger equation for this very purpose. Since then several authors [7] have studied his approach ignoring the fact that nature does not recognize such an equation. Indeed, the superposition principle which is at the very heart of quantum mechanics, and is a consequence of the linearity of the Schrödinger equation [8], has survived numerous tests [9–11] ruling out¹ nonlinear Schrödinger equations of various types [14, 15].

Nevertheless, the Kostin approach is an excellent source of inspiration to construct potentials which decelerate a Gaussian wave packet. In this sense the Kostin equation is an early representative of coherent control [16].

In the present article, we revisit the problem of extracting kinetic energy from a classical and a quantum particle with the help of appropriate potentials, and make the connection to nonlinear Schrödinger equations à la Kostin.

1.1 Deceleration of Particles: A Brief Overview

Arguably the field of deceleration of particles starts with the seminal experiments of Ernest Rutherford sending alpha particles through gold foils to probe the constitution of matter. This work leads us to a refined model of the atom, a first understanding of the nucleus and eventually to quantum mechanics. During his time with Rutherford Niels Bohr [17, 18] developed the first theoretical description of the stopping power of matter on a charged particle which was pushed further by an impressive list of physicists such as Hans Bethe, Felix Bloch, and Jens Lindhard [19]. It is not only central to nuclear physics but has also important applications in medicine. Indeed, the controlled deceleration of charged particles in cancer treatment relies on the rules of the stopping power [20].

The extraction of kinetic energy of an atomic beam with the help of a laser [21, 22] represents another milestone in the goal to decelerate and control quantum particles. It involves two crucial ingredients: (i) A detuning of the light frequency below the transition frequency, and (ii) spontaneous emission. Indeed, an atom moving against the laser makes a transition into its excited state by supplementing the laser energy by the kinetic energy. The spontaneous emission redistributes the energy taken out of the motion in one direction into all directions of space. The lowest

¹ We emphasize that this observation does not negate the existence of *effective* nonlinear Schrödinger equations, such as the Leggett equation [12] or the Gross-Pitaevskii equation [13] to describe the magnetization in liquid helium or a Bose-Einstein condensate of interacting atoms.

temperature achievable by the so-called Doppler cooling [23] is given by a balance of the extraction and the redistribution.

The techniques of Sisyphus cooling [24] and other advanced methods rely on similar principles: Decelerating forces combined with dissipation.

However, in particle physics the technique of stochastic cooling [25] does not rely on dissipation but on feedback. The information of the velocity distribution measured on one side of a storage ring is forwarded to the other side, and appropriate corrections of the velocity distribution are performed before the beam reaches again the measurement zone. A similar feedback mechanism has been proposed also in the field of cold atoms [26].

A completely different technique relies on applying external time- or position-dependent forces [27] provided by electric or magnetic fields [28–32] to slow down atomic or molecular beams. The method of delta-kick cooling [33–36] also falls into this category.

In the present article, we study a similar technique to decelerate atoms and reach a quantum state of the center-of-mass motion close to a momentum eigenstate of vanishing eigenvalue. Here we are guided by three observations: (i) The *nonlinear* Schrödinger equation of Kostin [6] decelerates [7] a Gaussian wave packet. (ii) We can find the potential necessary to decelerate the Gaussian according to the *linear* Schrödinger equation from the underlying mathematical identity [8]. (iii) These potentials are at most quadratic in the coordinate [37].

Needless to say, the opposite of the deceleration of a particle, that is its acceleration is also of great interest. Indeed, for atoms this phenomenon is achieved by moving lattices [38–41], and charged particles can experience quite a substantial acceleration using the wake field technique [42, 43]. Most interesting is also the approach of accelerating electrons with dielectric media and ultra-short laser pulses [44].

However, since the main topic of our article is the Kostin equation and the associated *deceleration* we concentrate ourselves on this topic but emphasize that our techniques also work for *acceleration* as briefly discussed in Appendix 1.

1.2 Outline

Our article is organized as follows:

In order to provide the foundations for our discussion of the Kostin equation we first recall in Sect. 2 the essential ingredients of a classical description of velocity-dependent damping. Here, we focus on the time evolution of the velocity and the coordinate of the particle. Due to the exponential time-dependence of the velocity, we find a linear relation between the coordinate and the velocity.

We then compare and contrast this dissipative force to a time-dependent non-dissipative one which is independent of the coordinate and show that it leads to a trajectory that is identical to the one resulting from the velocity-dependent damping. However, the required force depends on the initial velocity of the particle. The non-linearity of the Kostin equation is a remnant of this feature.

The associated exponential reduction in the kinetic energy is a consequence of the particle climbing a time-dependent *linear* potential and the transformation of kinetic into potential energy. We then show that a time-independent inverted parabolic potential achieves the same effect. Again the parameters of this potential such as the location of its center or the steepness depend on the motion representing a sense of nonlinearity.

So far our analysis was limited to a *single* particle. In Sect. 3, we address the problem of an *ensemble* of particles described by quantum theory. Here we switch from the Newton formalism to the Schrödinger equation. In particular, we determine for a moving Gaussian wave packet the potential which enforces the deceleration of the probability density according to the classical trajectory. Indeed, this potential is linear and quadratic in the coordinate with a position-independent but time-dependent off-set.

The linear part is identical to the one used for an exponential slow-down of a classical particle. However, the quadratic one depends on the time dependence of the width which is still at our disposal. Hence, we find infinitely many potentials which achieve this goal of deceleration. It is our choice of the asymptotic state that determines the time dependence of the quadratic part of the potential.

A *nonlinear* Schrödinger equation emerges for the very special time dependence of the width of the Gaussian wave packet which makes the phase of the wave function to be proportional to the potential. This unusual dynamics also requires a special time dependence of the position-independent off-set of the potential. In Sect. 4, we derive this equation and discuss its relation to the Kostin equation.

We then turn in Sect. 5 to the time evolution of a Gaussian wave packet due to the linear potential from the classical problem, and the quadratic one familiar from the Kostin equation. We visualize the resulting dynamics first in position space, and then in Wigner phase space. Since the Wigner function of a Gaussian is again a Gaussian we notice that the center of the Wigner function follows a straight line in phase space toward the position axis while its quadratures get squeezed. During this process the Gaussian is not aligned with the axes of phase space but slowly gets rotated by the time-dependent oscillator determining the width.

So far our considerations have focused exclusively on theoretical aspects and we have not touched questions related to possible experimental realisations of our ideas. In order to fill this gap we dedicate Sect. 6 to a discussion of this topic. Here we concentrate on two systems: surface gravity water waves and cold atoms. However, we emphasize that at this point our treatment is solely centered around the key ingredients and a more detailed analysis has to be postponed to a future article.

We conclude in Sect. 7 by summarizing our results and providing an outlook.

In order to focus on the central ideas while keeping the article self-contained we summarize lengthy calculations in appendices. Indeed, we dedicate Appendix 1 to the derivation of the time-dependent potential necessary to stop the moving Gaussian wave packet using the continuity equation and the quantum Hamilton-Jacobi equation. This calculation brings out most clearly the fact that our method works not only for an exponential deceleration but for an arbitrary prescribed center-of-mass motion. In particular, it also allows for an exponential acceleration.

Moreover, in Appendix 2 we diagonalize a general Gaussian Wigner function, that is we obtain an expression for its angle of orientation with respect to one axis of phase space. We also apply this formula to the Kostin dynamics and derive analytical expressions for the short- and long-time limit of the rotation angle.

A remarkable result of Appendix 2 is that the starting point of this decay of the rotation angle is $\pi/4$, whereas conventional wisdom predicts $\pi/2$. In order to resolve this small mystery we devote Appendix 3 to a phase space analysis of the free time-evolution of a symmetric Gaussian Wigner function, that is the transition from circular to ellipsoidal contour lines. We identify the origin of this symmetry breaking and rederive the short-time limit of the rotation angle from a variational principle.

2 Exponential Deceleration: Classical Particle

In the present section, we compare and contrast three techniques to decelerate a classical particle, whereas the first one relies on a *dissipative* force whose strength is governed by the instantaneous velocity, the second and third one result from *non-dissipative* forces which are either independent of, or linear in the coordinate. In the second case the homogeneous force is time-dependent but the third examples relies on a time-independent force. Although the three approaches are fundamentally different they yield an identical time dependence of the velocities and trajectories.

However, there is a subtle difference, whereas the first method is independent of the initial conditions, the success of the other two depends crucially on them.

2.1 Dissipative Force

The most elementary model of damping in classical mechanics employs the velocity-dependent force

$$F_d \equiv -\gamma mv \quad (1)$$

where γ and v denote the damping rate of the particle of mass m and the instantaneous velocity, respectively. In the remainder of this article we consider for the sake of simplicity a one-dimensional motion along the z -axis.

In the absence of other forces the Newton equation of motion

$$m \frac{d}{dt} v = -\gamma mv \quad (2)$$

immediately yields the well-known exponential damping

$$\bar{v}(t) = v_0 e^{-\gamma t} \quad (3)$$

of the initial velocity $\bar{v}(0) \equiv v_0$.

Hence, the kinetic energy

$$E_{\text{kin}}(t) \equiv \frac{m}{2} \bar{v}^2(t) = E_{\text{kin}}(0) e^{-2\gamma t} \quad (4)$$

decays with twice the rate γ starting from the initial kinetic energy $E_{\text{kin}}(0) \equiv mv_0^2/2$.

The relation

$$v = \frac{d}{dt} z \quad (5)$$

together with Eq. (3) immediately yields the trajectory

$$\bar{z}(t) = z_0 + v_0 \frac{1}{\gamma} (1 - e^{-\gamma t}) \quad (6)$$

where $\bar{z}(0) \equiv z_0$.

Hence, in the limit $t \rightarrow \infty$ the particle approaches the asymptotic velocity

$$v_\infty \equiv \lim_{t \rightarrow \infty} \bar{v}(t) = 0, \quad (7)$$

and thus comes to rest at the coordinate

$$z_\infty \equiv \lim_{t \rightarrow \infty} \bar{z}(t) \equiv z_0 + v_0 \frac{1}{\gamma}. \quad (8)$$

Next, we represent the trajectory, Eq. (6), in terms of the instantaneous velocity $\bar{v}(t)$ and the final coordinate z_∞ , given by Eqs. (3) and (8), and arrive at the linear relation

$$\bar{z}(t) = z_\infty - \bar{v}(t) \frac{1}{\gamma} \quad (9)$$

between the coordinate \bar{z} and the velocity \bar{v} .

We emphasize that this linearity is a consequence of the *exponential* damping. Indeed, upon differentiation an exponential function reproduces itself up to a constant. It is this very feature that allows us to express the exponential in \bar{z} given by Eq. (6) by \bar{v} , and obtain the linear connection Eq. (9).

2.2 Time-Dependent Homogeneous Force

In the preceding section, we have recalled the time dependence of the velocity as well as the coordinate of a particle exposed to a velocity-dependent *dissipative* force F_d . Here we have shown that independent of the initial conditions, that is, of its initial velocity, the particle comes to rest on a time scale governed by the inverse damping constant.

We now present this problem from a slightly different point of view and show that we get identical behaviors for velocity and coordinate when we expose the particle to a *non-dissipative* force F_h which is independent of the coordinate but explicitly time dependent. Moreover, in contrast to F_d the force F_h results from a potential but depends on the initial velocity of the particle.

2.2.1 Trajectory-Dependent Linear Potential

When we differentiate the velocity $\bar{v} = \bar{v}(t)$ given by Eq. (3) with respect to t we recognize that the particle experiences a time-dependent acceleration

$$\bar{a}(t) \equiv \frac{d}{dt}\bar{v}(t) \equiv -\gamma\bar{v}(t) \quad (10)$$

caused by the *dissipative* force F_d which is proportional to its instantaneous velocity $\bar{v}(t)$.

For this reason we obtain a velocity $\bar{v} = \bar{v}(t)$ and a trajectory $\bar{z} = \bar{z}(t)$ that are identical to the ones due to F_d by a time-dependent but *non-dissipative* force

$$F_h(t) \equiv ma_h(t) = -m\gamma\bar{v}(t) \quad (11)$$

whose acceleration a_h is governed by the instantaneous velocity $\bar{v}(t)$ caused by F_d and given by Eq. (3). Since F_h is independent of the coordinate z we deal with a homogeneous force as indicated by the subscript h .

Although on first sight the two Newton equations of motion, Eqs. (1) and (11), for F_d and F_h seem to be identical, they differ in a small but extremely important detail: In Eq. (1) the overbar of v is missing which makes F_d dependent on the dynamical variable v , and hence, independent of the initial velocity v_0 of the particle.

In contrast, F_h depends by virtue of Eq. (3) explicitly on v_0 , that is

$$F_h(t) = -m\gamma v_0 e^{-\gamma t}. \quad (12)$$

So far our discussion has centered around forces and the ensuing trajectories. However, we now turn to an analysis of the problem of deceleration of a particle from the point of view of a potential. This approach is possible since in the remainder of our article we deal with non-dissipative forces.

Moreover, the introduction of a potential allows us to connect our classical considerations to the quantum mechanical ones in Sect. 3 based on the Schrödinger equation. Indeed, quantum theory employs potentials rather than forces.

With the help of the relation

$$F_h = -\frac{d}{dz}V_1 \quad (13)$$

we can represent the homogeneous force F_h given by Eq. (11) by the derivative of a linear potential

$$V_1(z, t) \equiv m\gamma\bar{v}(t)z + \bar{V}_1(t) \quad (14)$$

whose slope depends on the instantaneous velocity $\bar{v}(t)$ of the particle, and the offset $\bar{V}_1 = \bar{V}_1(t)$ is purely time-dependent. Indeed, F_h is independent of $\bar{V}_1(t)$ because of the differentiation with respect to position.

Nevertheless, it is useful to consider the special choice

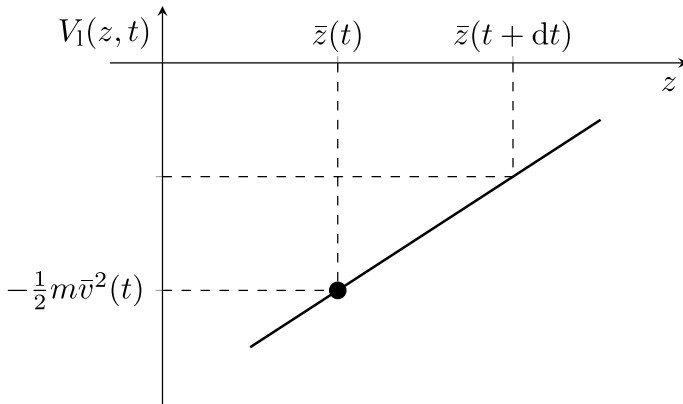


Fig. 1 Representation of the time-dependent linear potential $V_1 = V_1(z, t)$ given by Eq. (16) for a fixed moment in time. At the position $z = \bar{z}$ the particle feels a linear potential whose steepness is determined by its instantaneous velocity $\bar{v}(t)$. The value of $V_1(z = \bar{z}(t), t)$ at the position $z = \bar{z}$ of the particle is given by its negative kinetic energy

$$\bar{V}_1(t) \equiv -m\gamma\bar{v}(t)\bar{z}(t) - \frac{m}{2}\bar{v}^2(t), \tag{15}$$

which leads us to the total time-dependent linear potential

$$V_1(z, t) = m\gamma\bar{v}(t)[z - \bar{z}(t)] - \frac{m}{2}\bar{v}^2(t). \tag{16}$$

Hence, in the neighborhood of the position $z = \bar{z}$ of the particle, it feels a linear potential whose slope is governed by the velocity \bar{v} , and the value of V_1 is given by the negative kinetic energy $-m\bar{v}^2/2$, as shown in Fig. 1.

2.2.2 Climbing a Hill

In the framework of the linear potential V_1 , the exponential reduction of the kinetic energy given by Eq. (4) results from the continuous climbing of a hill whose instantaneous steepness and value adjust themselves to the instantaneous velocity and kinetic energy of the particle. In this process kinetic energy is continuously transferred into potential energy which for $t \rightarrow \infty$ vanishes.

We gain deeper insight into this mechanism of decelerating a particle by determining the change

$$dV_1 \equiv V_1[\bar{z}(t + dt), t + dt] - V_1[\bar{z}(t), t] \tag{17}$$

in potential energy during the infinitesimal time interval dt due to the approximately linear motion

$$\bar{z}(t + dt) \cong \bar{z}(t) + \bar{v}(t) dt, \tag{18}$$

and analyzing the explicit dependence of V_1 on time, that is

$$dV_1 = \left(\frac{\partial V_1}{\partial z} \frac{dz}{dt} + \frac{\partial V_1}{\partial t} \right) \Big|_{z=\bar{z}} dt. \quad (19)$$

We start by discussing the partial time derivative of V_1 and obtain from the definition, Eq. (16), of V_1 the identity

$$\frac{\partial V_1}{\partial t} \Big|_{z=\bar{z}} = m\gamma \left(\frac{d}{dt} \bar{v} \right) (z - \bar{z}) \Big|_{z=\bar{z}} - m\gamma \bar{v}^2 - m\bar{v} \frac{d}{dt} \bar{v}, \quad (20)$$

where we have used Eq. (5).

Obviously, the first contribution vanishes for $z = \bar{z}$, and with the help of the expression, Eq. (10), for the time-dependent acceleration we arrive at

$$\frac{\partial V_1}{\partial t} \Big|_{z=\bar{z}} = 0. \quad (21)$$

Hence, the explicit time dependence of V_1 does not contribute to the change dV_1 of the potential energy. There are two reasons for this feature which we can trace back to the construction of V_1 in Eq. (16), that is to the choice of \bar{V}_1 given by Eq. (15): (i) V_1 is centered at the trajectory $\bar{z} = \bar{z}(t)$ of the particle, and (ii) the value of V_1 at $z = \bar{z}$ is the negative instantaneous kinetic energy.

In addition, two properties of the motion enter into the derivation of Eq. (21): (i) the time rate of the change in the coordinate is the velocity, and (ii) the time rate of the velocity is proportional to the velocity. Whereas (i) always holds true, the feature (ii) is a consequence of the exponential time dependence of \bar{v} .

Finally, we address the first term in Eq. (19) and find from the definition, Eq. (16), of V_1 the relation

$$\frac{\partial V_1}{\partial z} \Big|_{z=\bar{z}} = \frac{\partial V_1}{\partial z} = m\gamma \bar{v}. \quad (22)$$

We emphasize that in contrast to the partial derivative of V_1 with respect to time, Eq. (21), we do not have to evaluate the derivative with respect to the coordinate at the trajectory $z = \bar{z}$ as expressed by Eq. (22). Indeed, this feature is a consequence of the homogeneous force, that is the derivative of V_1 which leads to the force is independent of the coordinate.

When we substitute Eqs. (21) and (22) into Eq. (19), the change

$$dV_1 = m\gamma \bar{v}^2(t) dt \quad (23)$$

in the potential energy is due to the kinetic energy, that is

$$dV_1 = 2\gamma E_{\text{kin}} dt \quad (24)$$

where we have recalled Eq. (4).

Equation (21) shows that along the trajectory $z = \bar{z}$ the explicit time dependence of V_1 vanishes. As a result, during an infinitesimal time period dt the particle climbs a time-independent hill as indicated in Fig. 1 and the total energy

$$E \equiv E_{\text{kin}} + V_1 \quad (25)$$

is conserved, that is

$$0 = dE = dE_{\text{kin}} + dV_1. \quad (26)$$

Hence, we find the connection

$$dE_{\text{kin}} = -dV_1 \quad (27)$$

between the changes dE_{kin} and dV_1 in kinetic and potential energies. Indeed, the growth of one is at the expense of the other.

When we apply the argument of energy conservation, Eqs. (24)–(27), we arrive at the differential equation

$$\frac{d}{dt}E_{\text{kin}} = -2\gamma E_{\text{kin}}, \quad (28)$$

whose solution is in complete agreement with Eq. (4) derived from the dissipative force F_d .

Hence, the time-dependent linear potential V_1 given by Eq. (16) leads to an exponential reduction in the kinetic energy of the particle. Obviously here we do not employ a dissipative force but the extraction is the result of the time-dependent potential determined by the desired motion.

We emphasize that this derivation also brings out most clearly that our choice, Eq. (15), of the position-independent off-set $\bar{V}_1(t)$ plays a crucial role in the vanishing of the contribution to dV_1 , Eq. (21), due to the time dependence of V_1 . As a result, during dt the particle runs up a linear ramp whose slope does not change as shown in Fig. 1.

We conclude our discussion of this mechanism of decelerating a particle by noting that the total energy

$$E \Big|_{z=\bar{z}} = (E_{\text{kin}} + V_1) \Big|_{z=\bar{z}} = 0 \quad (29)$$

along the trajectory $z = \bar{z}$ vanishes for all times. This property is again a consequence of the construction of V_1 , given by Eq. (16), and, in particular, of the fact that the kinetic energy $E_{\text{kin}} = \bar{v}^2/(2m)$ is canceled by the value of V_1 at $z = \bar{z}$.

2.2.3 Phase Space Trajectory

In our analysis of the second example of a non-dissipative force to slow down a particle presented in the next section, and employing an inverted harmonic oscillator potential we shall return to the property of a vanishing total energy expressed by Eq. (29). Indeed, we shall observe that this condition puts the particle onto one of the separatrices of the associated phase space enforcing the exponential deceleration along a *straight* phase space trajectory.

However, in our discussion of the dissipative force we have already noted that the exponential dependence of the velocity on time enforces a linear relationship between the coordinate and the velocity as expressed by Eq. (9). Therefore, it is tempting to think that this linearity also predicts a straight phase space trajectory. In order to avoid the complications associated with the notion of phase space for a dissipative system we have not addressed this feature in Sect. 2.1.

Since we now deal with a non-dissipative system we do not have these problems anymore, and indeed in a phase space spanned by z and $p \equiv mv$ the trajectory

$$p = -m\gamma(z - z_\infty) \quad (30)$$

is a straight line connecting the points (z_0, mv_0) and $(z_\infty, 0)$ with a slope $-\gamma$. In Sect. 5.3 we shall verify this feature using the Wigner phase space distribution [1].

2.3 Inverted Harmonic Oscillator

In the preceding section, we have shown that a time-dependent homogeneous force leads to an exponential reduction in the kinetic energy of the particle which is indistinguishable from that of a dissipative force. In the present section, we show that an appropriately designed time-independent inverted parabolic potential V_{io} achieves the same goal. For this purpose, we first motivate the form of the potential using the linear connection, Eq. (9), between coordinate and velocity. We then solve the equations of motion corresponding to V_{io} and arrive at the expressions, Eqs. (3) and (6), for the time-dependent velocity and coordinate.

2.3.1 Heuristic Argument for the Shape of the Potential

We start by using Eq. (9) to express the kinetic energy in terms of the trajectory $\bar{z}(t)$ rather than the instantaneous velocity $\bar{v}(t)$, and find the representation

$$E_{\text{kin}}(t) = \frac{m}{2}\gamma^2[\bar{z}(t) - z_\infty]^2. \quad (31)$$

Indeed, due to the quadratic dependence, Eq. (4), of E_{kin} on \bar{v} , and the linear dependence, Eq. (9), of \bar{z} on \bar{v} , we obtain a *quadratic* dependence of E_{kin} on \bar{z} .

This feature suggests to study the motion of the particle in an inverted harmonic oscillator potential

$$V_{\text{io}}(z) \equiv -\frac{m}{2}\gamma^2(z - z_\infty)^2 \quad (32)$$

centered at z_∞ whose steepness is governed by the damping rate γ .

Indeed, at z_0 the potential energy

$$V_{\text{io}}(z_0) = -\frac{m}{2}v_0^2 \equiv -E_{\text{kin}}(0) \quad (33)$$

is the negative initial kinetic energy of the particle. Here we have recalled the definition, Eq. (8), of z_∞ .

Hence, the total initial energy

$$E \equiv E_{\text{kin}}(0) + V_{\text{io}}(z_0) = 0 \quad (34)$$

vanishes, and due to the conservative potential, E is conserved. As the particle climbs the parabolic barrier it loses its kinetic energy. Since according to Eq. (32) we have $V(z_\infty) = 0$ and the total energy vanishes, the asymptotic kinetic energy must vanish as well.

2.3.2 Resulting Trajectory

We now show that the expressions for the velocity and coordinate of the particle in the inverted harmonic oscillator are identical to those obtained from the dissipative force, Eq. (1).

For this purpose, we study the Newton equation of motion

$$\ddot{z} - \gamma^2 z = -\gamma^2 z_\infty \quad (35)$$

resulting from the potential V_{io} given by Eq. (32).

The general solution

$$z(t) = z_+ e^{\gamma t} + z_- e^{-\gamma t} + z_\infty \quad (36)$$

of Eq. (35) consisting of a linear combination of a growing and a decaying exponential is determined by the constants z_+ and z_- of integration. They follow from the initial conditions z_0 and v_0 and result in the trajectory

$$\bar{z}(t) = \frac{1}{2} \left(z_0 + \frac{v_0}{\gamma} - z_\infty \right) e^{\gamma t} + \frac{1}{2} \left(z_0 - \frac{v_0}{\gamma} - z_\infty \right) e^{-\gamma t} + z_\infty. \quad (37)$$

With the help of the definition Eq. (8), we eliminate the growing exponential and arrive at

$$\bar{z}(t) = z_\infty - v_0 e^{-\gamma t} \frac{1}{\gamma}, \quad (38)$$

that is the trajectory given by Eq. (9).

2.3.3 Connection Between the Two Non-dissipative Forces

We conclude this discussion of the inverted harmonic oscillator by noting a close connection between the time-dependent linear and the time-independent inverted parabolic potential. Indeed, when we subtract the trajectory \bar{z} from the dynamical variable z in the potential V_{io} of the inverted harmonic oscillator, and add it again, use the representation, Eq. (8), of \bar{z} , and undo the square we establish the identity

$$V_{\text{io}}(z) = V_1(z, t) + \delta V(z, t). \quad (39)$$

Hence, the time-independence of V_{io} is the result of the additional inverted parabolic potential

$$\delta V(z, t) \equiv -\frac{1}{2}m\gamma^2(z - \bar{z})^2 \quad (40)$$

whose time dependence originates from the fact that the center of the parabolic potential is governed by the trajectory $\bar{z} = \bar{z}(t)$.

It is interesting to note that the force at the position \bar{z} of a particle in the inverted harmonic parabolic potential and in the linear one are identical, since

$$-\frac{d}{dz}\delta V \Big|_{z=\bar{z}} = m\gamma^2(z - \bar{z}) \Big|_{z=\bar{z}} = 0, \quad (41)$$

that is the force resulting from δV vanishes at the position of the particle.

We shall return to the potential δV in the next section when we discuss the deceleration of a *quantum* particle. Here we have in the width of the wave packet an additional parameter which will allow us to include δV , and arrive at the time-independent inverted harmonic oscillator potential V_{io} given by Eq. (32) to exponentially slow down the particle.

3 Exponential Deceleration: Quantum Particle

In the preceding section we have compared and contrasted the slowing down of a single classical particle due to two different types of forces: (i) a dissipative one, and (ii) non-dissipative but time-dependent forces. In this section, we extend these considerations to quantum mechanics, and discuss the problem of the deceleration of a moving Gaussian wave packet

$$\psi(z, t = 0) \equiv \frac{1}{\sqrt[4]{\pi}} \sqrt{\frac{1}{\Delta z(0)}} \exp \left\{ -\frac{1}{2} \left[\frac{z - \bar{z}(0)}{\Delta z(0)} \right]^2 \right\} e^{im\bar{v}(0)[z - \bar{z}(0)]/\hbar} \quad (42)$$

with the initial width

$$\Delta z(t = 0) \equiv \Delta z(0) \quad (43)$$

according to the Schrödinger equation.

We first analyze the required potential and the associated phase of the wave function. Then we study special choices of the time-dependence of the width $\Delta z = \Delta z(t)$ which determines the asymptotic quantum state. Moreover, we briefly discuss the influence of a solely time-dependent contribution to the potential as well as the phase which will play a crucial role in the next section in obtaining a nonlinear Schrödinger equation à la Kostin.

3.1 Potential and Phase

In Appendix 1 we show that the combination

$$V(z, t) \equiv V_2(z, t) + V_1(z, t) + V_0(t) \quad (44)$$

of potentials consisting of V_1 given by Eq. (16), and

$$V_2(z, t) \equiv -\frac{m}{2} \frac{1}{\Delta z(t)} \left[\left(\frac{d^2}{dt^2} \Delta z \right) - \frac{\hbar^2}{m^2} \frac{1}{\Delta z^3(t)} \right] [z - \bar{z}(t)]^2 \quad (45)$$

as well as

$$V_0(t) \equiv m\bar{v}^2 - \frac{d}{dt}s - \frac{\hbar^2}{2m} \frac{1}{\Delta z^2(t)} \quad (46)$$

with a time-dependent function $s = s(t)$, creates with the help of the Schrödinger equation

$$i\hbar \frac{\partial}{\partial t} \psi = -\frac{\hbar^2}{2m} \frac{\partial^2}{\partial z^2} \psi + V\psi \quad (47)$$

a probability density

$$W(z, t) = |\psi(z, t)|^2 = \frac{1}{\sqrt{\pi}} \frac{1}{\Delta z(t)} \exp \left\{ -\left[\frac{z - \bar{z}(t)}{\Delta z(t)} \right]^2 \right\} \quad (48)$$

whose center follows the classical trajectory $z = \bar{z}(t)$ given by Eq. (6).

In this case the wave function

$$\psi(z, t) \equiv \sqrt{W(z, t)} e^{iS(z, t)/\hbar} \quad (49)$$

with the probability density W defined by Eq. (48) and the action

$$S(z, t) \equiv \frac{m}{2} \frac{1}{\Delta z(t)} \left(\frac{d}{dt} \Delta z(t) \right) [z - \bar{z}(t)]^2 + m\bar{v}(t)[z - \bar{z}(t)] + s(t) \quad (50)$$

is a solution of the Schrödinger equation, Eq. (47), in the presence of the potential V with the initial condition Eq. (42), provided

$$s(t = 0) = 0 \quad (51)$$

and

$$\left. \frac{d}{dt} \Delta z \right|_{t=0} = 0. \quad (52)$$

From Eq. (44), we recognize three contributors to V : (i) the linear potential V_1 defined by Eq. (16) and used in the preceding section to decelerate a *classical* particle, (ii) a parabolic potential given by Eq. (45) whose steepness is determined by

the time-dependence of the width $\Delta z = \Delta z(t)$ of the wave packet, and (iii) a time-dependent off-set V_0 governed according to Eq. (46) by \bar{v} , ds/dt and Δz .

3.2 Special Examples

So far our considerations have been rather general. In particular, we have not found a condition specifying the time-dependence of Δz , nor of s . We now discuss examples of these functions and make in this way the connection to the field of coherent control. Indeed, the choice of Δz determines the final wave function.

We start with s and note that the function

$$s^{(0)}(t) \equiv \int_0^t dt' \left[m\bar{v}^2(t') - \frac{\hbar^2}{2m} \frac{1}{\Delta z^2(t')} \right] \quad (53)$$

which satisfies the initial condition, Eq. (51), eliminates the off-set V_0 , that is $V_0(t) \equiv 0$.

Moreover, the freedom in the time dependence of Δz allows us to select special asymptotic states when the center of the wave packet has come to rest, that is for $t \rightarrow \infty$.

For the example of a Gaussian time dependence

$$\Delta z^{(G)}(t) \equiv \Delta z(0)e^{-(\gamma t)^2}, \quad (54)$$

the wave packet at rest at z_∞ has a vanishing width in position space and therefore approximates² a position eigenstate at z_∞ . Here we have included in $\Delta z^{(G)}$ the superscript G as to reflect the fact that we have selected the very specific time dependence of the decaying Gaussian given by Eq. (54). We note that Eq. (54) satisfies the initial conditions, Eqs. (43) and (52), for Δz .

The associated parabolic potential

$$V_2^{(G)}(z, t) = \frac{m}{2} \left\{ 2\gamma^2 [1 - 2(\gamma t)^2] + \frac{\hbar^2}{m^2 [\Delta z(0)]^4} e^{4(\gamma t)^2} \right\} [z - \bar{z}(t)]^2 \quad (55)$$

following from Eq. (45) turns, in the course of time, into a binding one, and becomes infinitely steep for $t \rightarrow \infty$ enforcing the localization of the particle at z_∞ .

On the other hand, the time dependence

$$\Delta z^{(c)}(t) \equiv \Delta z(0) \cosh(\gamma t) \quad (56)$$

of the width which also satisfies the initial conditions, Eqs. (43) and (52), leads to an approximate momentum eigenstate of vanishing eigenvalue due to the inverted harmonic oscillator potential

² We emphasize that even an infinitely narrow Gaussian in position space is only an *approximation* of a position eigenstate which is normalized with respect to a delta function, in sharp contrast to the Gaussian which is properly normalized.

$$V_2^{(c)}(z, t \rightarrow \infty) \cong -\frac{1}{2}m\gamma^2[z - \bar{z}(t)]^2 \quad (57)$$

emerging in the asymptotic limit. Here we have neglected the second contribution in V_2 due to $[\Delta z(t)]^{-3}$ since it approaches zero in an exponential time. Moreover, we also emphasize that the infinitely wide Gaussian which is normalized, only serves as an approximation of a non-normalizable momentum eigenstate.

We conclude this discussion of the role of the time dependence of the width by returning to the time-independent inverted harmonic oscillator analyzed classically in Sect. 2.3. Indeed, when we require the differential equation

$$\frac{d^2}{dt^2} \Delta z^{(io)} - \gamma^2 \Delta z^{(io)} - \frac{\hbar^2}{m^2} \frac{1}{[\Delta z^{(io)}]^3} = 0, \quad (58)$$

the quadratic contribution V_2 to V given by Eq. (45) reduces to δV centered around the *time-dependent* trajectory $\bar{z} = \bar{z}(t)$ and defined by Eq. (40), that is

$$V_2^{(io)} = \delta V, \quad (59)$$

and the complete potential V of Eq. (44) is indeed the *time-independent* inverted harmonic oscillator potential V_{io} of Eq. (32). Here we have made use of Eq. (39).

4 Nonlinear Schrödinger Equation à la Kostin

In the preceding section we have shown that the time dependence of Δz governs the quadratic part V_2 of the potential V which decelerates the Gaussian wave packet, and determines the asymptotic state. We dedicate the present section to a special time dependence of Δz which together with another one of s makes the potential V proportional to the phase of the wave function.

In this way we arrive at the nonlinear Schrödinger equation

$$i\hbar \frac{\partial}{\partial t} \psi = -\frac{\hbar^2}{2m} \frac{\partial^2}{\partial z^2} \psi + \hbar\gamma \frac{1}{2i} \ln \left(\frac{\psi}{\psi^*} \right) \psi \quad (60)$$

which is closely related to an equation to describe damping in quantum mechanics proposed exactly 50 years ago by Kostin [6]. We first derive Eq. (60) from the results of the preceding section, and then discuss the relationship with the Kostin equation.

4.1 Derivation

We start our analysis by noting that the phase of the wave function and the potential are intimately connected by the quantum Hamilton-Jacobi equation as discussed in detail in Ref. [8] and in Appendix 1. However, for the example of a Gaussian wave packet the connection stands out most clearly. Indeed, when we compare the individual terms in V given by Eq. (44), and in S of Eq. (50), we find a great similarity.

In order to facilitate this comparison we recall here the explicit expressions for the potential

$$\begin{aligned}
 V = & -\frac{m}{2} \frac{1}{\Delta z} \left(\frac{d^2}{dt^2} \Delta z - \frac{\hbar^2}{m^2} \frac{1}{\Delta z^3} \right) (z - \bar{z})^2 \\
 & + m\gamma \bar{v}(z - \bar{z}) \\
 & + \frac{1}{2} m \bar{v}^2 - \frac{d}{dt} s - \frac{\hbar^2}{2m} \frac{1}{\Delta z^2}
 \end{aligned} \tag{61}$$

and the action

$$S = \frac{m}{2} \frac{1}{\Delta z} \left(\frac{d}{dt} \Delta z \right) (z - \bar{z})^2 + m\bar{v}(z - \bar{z}) + s. \tag{62}$$

We find that the terms linear in z in V and S are proportional to each other with the decay constant γ , whereas the corresponding quadratic contributions are obviously different in form.

However, the requirement

$$\frac{d^2}{dt^2} \Delta z^{(P)} - \frac{\hbar^2}{m^2 (\Delta z^{(P)})^3} = -\gamma \frac{d}{dt} \Delta z^{(P)} \tag{63}$$

for the time dependence of the width $\Delta z^{(P)} = \Delta z^{(P)}(t)$ represented by the Pinney equation, Eq. (63), transforms V_2 given by Eq. (45) into

$$V_2^{(P)}(z, t) \equiv \frac{m}{2} \gamma \frac{1}{\Delta z^{(P)}(t)} \left(\frac{d}{dt} \Delta z^{(P)}(t) \right) [z - \bar{z}(t)]^2 \tag{64}$$

which is up to γ the quadratic contribution to S . Here we have included a superscript P in $\Delta z^{(P)}$ and $V_2^{(P)}$ as to reflect the fact that both are governed by the time-dependence of the Pinney equation, Eq. (63).

Moreover, when we subject s to the differential equation

$$\frac{1}{2} m \bar{v}^2 - \frac{d}{dt} s^{(P)} - \frac{\hbar^2}{2m} \frac{1}{(\Delta z^{(P)})^2} = \gamma s^{(P)} \tag{65}$$

with the solution

$$s^{(P)}(t) = \int_0^t dt' e^{-\gamma(t-t')} \left[\frac{1}{2} m \bar{v}^2(t') - \frac{\hbar^2}{2m} \frac{1}{[\Delta z^{(P)}(t')]^2} \right] \tag{66}$$

satisfying the initial condition, Eq. (51), we arrive at the relation

$$V^{(P)} = \gamma S^{(P)} \tag{67}$$

where

$$S^{(P)} \equiv \frac{m}{2} \frac{1}{\Delta z^{(P)}} \left(\frac{d}{dt} \Delta z^{(P)} \right) (z - \bar{z})^2 + m\bar{v}(z - \bar{z}) + s^{(P)}. \quad (68)$$

Hence, with the time dependence of $\Delta z^{(P)}$ and $s^{(P)}$ determined by the differential equations, Eqs. (63) and (65), the wave function

$$\psi \equiv \sqrt{W^{(P)}} \exp\left(\frac{i}{\hbar} S^{(P)}\right) \quad (69)$$

satisfies the nonlinear Schrödinger equation, Eq. (60). Here

$$W^{(P)}(z, t) \equiv \frac{1}{\sqrt{\pi}} \frac{1}{\Delta z^{(P)}(t)} \exp\left\{-\left[\frac{z - \bar{z}(t)}{\Delta z^{(P)}(t)}\right]^2\right\} \quad (70)$$

is given by Eq. (48) with Δz being replaced by $\Delta z^{(P)}$.

4.2 Kostin Equation

Two ingredients made it possible to achieve in the previous section the proportionality, Eq. (67), of $S^{(P)}$ and $V^{(P)}$: (i) The time dependence of $\Delta z^{(P)}$ given by the Pinney equation, Eq. (63), and (ii) the time dependence of $s^{(P)}$ determined by the differential equation, Eq. (65). In the present section we first show that this proportionality still holds true when we add to the potential $V^{(P)}$ a time-dependent off-set. This non-uniqueness is a consequence of the freedom in the function s .

We then address the original Kostin equation which contains as an additional potential the expectation value of the phase of the wave function. However, due to the non-uniqueness discussed before we can eliminate this term and arrive at the nonlinear Schrödinger equation, Eq. (60).

4.2.1 Non-uniqueness of Potential

We now address the following situation: We keep the time dependence of Δz governed by the Pinney equation, since it guarantees the proportionality of the quadratic contributions to the potential and the action. However, we add a position-independent but time-dependent off-set $\tilde{V}_0 = \tilde{V}_0(t)$ to the potential V arriving at

$$\tilde{V} \equiv V_2^{(P)} + m\gamma\bar{v}(z - \bar{z}) + \tilde{V}_0 + \frac{1}{2}m\bar{v}^2 - \frac{d}{dt}s - \frac{\hbar^2}{2m} \frac{1}{(\Delta z^{(P)})^2}. \quad (71)$$

The following question arises: Is it still possible to achieve the proportionality between the modified potential \tilde{V} and a new action \tilde{S} ?

The answer is affirmative since in \tilde{V} given by Eq. (71) we have not specified s yet. Indeed, the choice

$$\tilde{s}(t) \equiv \int_0^t dt' e^{-\gamma(t-t')} \left[\frac{1}{2} m \bar{v}^2(t') - \frac{\hbar^2}{2m} \frac{1}{[\Delta z^{(P)}(t')]^2} + \tilde{V}_0(t') \right] \quad (72)$$

ensures the relation

$$\tilde{V} = \gamma \tilde{S} \quad (73)$$

connecting the potential \tilde{V} given by Eq. (71) and the action

$$\tilde{S} \equiv \frac{m}{2} \frac{1}{\Delta z^{(P)}} \left(\frac{d}{dt} \Delta z^{(P)} \right) (z - \bar{z})^2 + m \bar{v} (z - \bar{z}) + \tilde{s}. \quad (74)$$

As a result, the wave function

$$\tilde{\psi} \equiv \sqrt{W^{(P)}} \exp \left(\frac{i}{\hbar} \tilde{S} \right) \quad (75)$$

also satisfies the nonlinear Schrödinger equation, Eq. (60).

This calculation demonstrates that the initial condition of the wave function does not suffice to uniquely determine the solution of the nonlinear Schrödinger equation, Eq. (60). Indeed, we can always add a position-independent but time-dependent offset to the potential and absorb the change in the function s .

4.2.2 Elimination of Expectation Value

This observation is relevant to the discussion of the Kostin equation [6] which is slightly different from the nonlinear Schrödinger equation, Eq. (60). Indeed, Kostin subtracts [6] from the potential term given by the phase of the wave function its expectation value. Hence, the Kostin equation for a wave function ψ_K in the presence of an arbitrary potential V_a reads

$$i\hbar \frac{\partial}{\partial t} \psi_K = -\frac{\hbar^2}{2m} \frac{\partial^2}{\partial z^2} \psi_K + [V_a + V_K - \langle V_K \rangle] \psi_K \quad (76)$$

where

$$V_K \equiv \hbar\gamma \frac{1}{2i} \ln \left(\frac{\psi_K}{\psi_K^*} \right) \quad (77)$$

and

$$\langle V_K \rangle \equiv \int_{-\infty}^{\infty} dz V_K(z, t) |\psi_K(z, t)|^2. \quad (78)$$

We emphasize that in general $\langle V_K \rangle$ creates an additional nonlinearity in Eq. (76). Since V_K depends on ψ_K , the expectation value $\langle V_K \rangle$ which also contains the probability density involves the wave function and its complex conjugate four times: According to Eq. (77) the potential V_K brings in the ratio ψ_K/ψ_K^* , and the probability density averaging V_K consists of $|\psi_K|^2 = \psi_K^* \psi_K$.

For this reason it is in general not possible to eliminate the term $\langle V_K \rangle$ which is obviously independent of the coordinate but may depend on time by a phase transformation.

However, for a Gaussian wave function and $V_a = 0$ this nonlinearity is trivial since we find from the definition, Eq. (77), of V_K , and the Kostin wave function

$$\psi_K \equiv \sqrt{W^{(P)}} e^{iS_K/h} \tag{79}$$

with the probability density $W^{(P)}$ given by Eq. (70) and the action

$$S_K \equiv \frac{m}{2} \frac{1}{\Delta z^{(P)}} \frac{d}{dt} (\Delta z^{(P)})(z - \bar{z})^2 + m\bar{v}(z - \bar{z}) + s_K \tag{80}$$

recalling the elementary integral relations

$$\int_{-\infty}^{\infty} dz W^{(P)} = 1 \text{ and } \int_{-\infty}^{\infty} dz (z - \bar{z}) W^{(P)} = 0 \tag{81}$$

as well as

$$\int_{-\infty}^{\infty} dz (z - \bar{z})^2 W^{(P)} = \frac{1}{2} (\Delta z^{(P)})^2 \tag{82}$$

the expression

$$\langle V_K \rangle = \gamma \langle S_K \rangle = \frac{m}{4} \gamma (\Delta z^{(P)}) \frac{d}{dt} \Delta z^{(P)} + \gamma s_K, \tag{83}$$

that is a position-independent off-set which we can absorb in the function s_K .

Hence, for the problem of a decelerating Gaussian we can always eliminate $\langle V_K \rangle$ and work with the nonlinear Schrödinger equation, Eq. (60).

5 Exponential Deceleration à la Kostin

In the preceding section, we have shown that the special choice, Eq. (63), of the time-dependence of the width of the Gaussian wave packet combined with the requirement Eq. (65) for s leads us to the nonlinear Schrödinger equation, Eq. (60). In the remainder of our article we analyze the quantum dynamics of a Gaussian wave packet governed by the *linear* Schrödinger equation, Eq. (47), with potentials motivated by the Kostin equation.

5.1 Formulation of the Problem

Indeed, we start from the combination

$$V(z, t) = \frac{1}{2} m \omega^2(t) [z - \bar{z}(t)]^2 + m \gamma \bar{v}(t) [z - \bar{z}(t)] - \frac{m}{2} \bar{v}^2(t) \tag{84}$$

of potentials where the quadratic part is represented by a time-dependent harmonic oscillator of frequency

$$\omega(t) \equiv \sqrt{\gamma \frac{1}{\Delta z(t)} \left(\frac{d}{dt} \Delta z(t) \right)} \quad (85)$$

and $\Delta z = \Delta z(t)$ follows from the Pinney equation

$$\frac{d^2}{dt^2} \Delta z + \gamma \frac{d}{dt} \Delta z = \frac{\hbar^2}{m^2} \frac{1}{\Delta z^3} \quad (86)$$

subjected to the initial conditions

$$\Delta z(t=0) = \Delta z(0) \quad (87)$$

and

$$\left. \frac{d}{dt} \Delta z \right|_{t=0} = 0. \quad (88)$$

Throughout this section we suppress for the sake of simplicity in notation the superscript P.

Hence, we use the time-dependence of Δz which is necessary to arrive at the non-linear Schrödinger equation but still require the cancellation of the time-dependent off-set V_0 defined by Eq. (46) using the expression, Eq. (53), for $s^{(0)}$ as to regain V_1 given by Eq. (16).

In this case the wave function

$$\psi \equiv \sqrt{W^{(P)}} \exp\left(\frac{i}{\hbar} S^{(P0)}\right) \quad (89)$$

with the probability density $W^{(P)}$ given by Eq. (70), and the action

$$S^{(P0)} \equiv \frac{m}{2} \frac{1}{\Delta z^{(P)}} \left(\frac{d}{dt} \Delta z^{(P)} \right) (z - \bar{z})^2 + m\bar{v}(z - \bar{z}) + s^{(0)} \quad (90)$$

solves the linear Schrödinger equation in the presence of the potential V given by Eq. (84).

5.2 Dynamics in Position Space

We devote the present section to an analysis of the potential V given by Eq. (84), and the resulting dynamics. In particular, we first derive approximate but analytical expressions for the time dependence of Δz as well as ω , and then compare and contrast them to the exact numerical solution of the Pinney equation, Eq. (86), as well as the resulting curve for ω following from the definition Eq. (85) of ω . This approach allows us to analyze the time scales in the individual contributions to V . We conclude by discussing the deceleration of the Gaussian wave packet in position space.

5.2.1 Potentials

We start with a discussion of the potential V given by Eq. (84) and note that V is made up of *three* time-dependent contributions: (i) a binding harmonic oscillator potential, (ii) a linear potential, and (iii) a coordinate-independent off-set.

Both the linear and the quadratic potential are centered at the instantaneous coordinate $z = \bar{z}(t)$ of the classical particle. Moreover, the slope of the linear potential and its off-set are governed by the instantaneous velocity $\bar{v}(t)$ and the negative kinetic energy $-E_{\text{kin}}(t)$ defined by Eqs. (3) and (4). Both quantities decay exponentially in time as shown in Fig. 2a.

However, the time dependence of the frequency $\omega = \omega(t)$ of the parabolic potential given by Eq. (85) is more complicated as shown in Fig. 2b. It follows from the width $\Delta z = \Delta z(t)$ of the Gaussian wave packet governed by the Pinney equation, Eq. (86), together with the initial conditions Eqs. (87) and (88).

In Fig. 2c we display in a double-logarithmic plot the numerically obtained time dependence of Δz and identify three features: (i) Δz increases monotonically without a bond, (ii) this growth is first linear in t , and (iii) then turns into one with the scaling $t^{1/4}$.

These two distinct power laws follow from approximate but analytic solutions of the Pinney equation, Eq. (86). Indeed, in the limit $\gamma t \ll 1$ we can neglect the first derivative of Δz in time, and the function

$$\Delta z(t) \cong \left[\Delta z^2(0) + \frac{\hbar^2}{m^2} \frac{t^2}{\Delta z^2(0)} \right]^{\frac{1}{2}} \quad (91)$$

is a solution of the resulting approximate differential equation

$$\frac{d^2}{dt^2} \Delta z \cong \frac{\hbar^2}{m^2} \frac{1}{\Delta z^3} \quad (92)$$

subjected to the initial conditions, Eqs. (87) and (88).

In Fig. 2c we depict by the dashed green line the time dependence of Δz given by the analytical expression Eq. (91). We emphasize that for short times this curve is an excellent approximation of the exact numerical result shown by the black solid line.

In the other extreme, that is for $1 \ll \gamma t$, we neglect the second derivative of Δz with respect to time, and the corresponding approximate Pinney equation

$$\gamma \frac{d}{dt} \Delta z \cong \frac{\hbar^2}{m^2} \frac{1}{\Delta z^3} \quad (93)$$

enjoys the asymptotic solution

$$\Delta z(t) \cong \sqrt{\frac{2\hbar}{\sqrt{\gamma m}}} \sqrt[4]{t} \quad (94)$$

as confirmed by the gray dotted line in Fig. 2c.

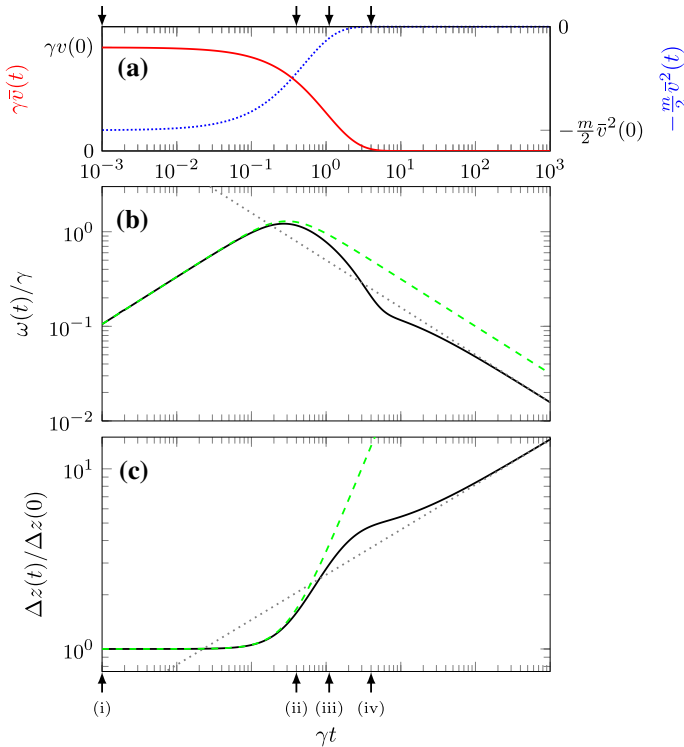


Fig. 2 Time scales in the three contributions **(a)**, **(b)** to the potential V given by Eq. (84) and in the width **(c)** of the decelerating Gaussian wave packet. **(a)** Slope and off-set of the linear potential given by $\gamma \bar{v}$ and the negative kinetic energy decay exponentially. **(b)** The time-dependent frequency $\omega = \omega(t)$ of the harmonic oscillator obtained by the numerical integration of Eq. (86) and represented by the solid black line first increases as $t^{1/2}$ but then decreases as $t^{-1/2}$, as verified by the asymptotic expressions, Eqs. (95) and (99), depicted by the dashed green and dotted gray curves, respectively. **(c)** The two distinct time scales in the time evolution of the width $\Delta z = \Delta z(t)$ described by the Pinney equation, Eq. (86). The dashed green line shows the approximate analytical solution for $\gamma t \ll 1$ as given by Eq. (91) which corresponds to the familiar spreading of the Gaussian wave packet linear in t . The dotted gray line shows the asymptotic solution for $\gamma t \gg 1$ given by Eq. (94) and growing as $t^{1/4}$. The solid line represents the numerical integration of Eq. (86). In the range $\gamma t \approx 1$, the wave packet experiences a phase of drastically reduced growth rate before it approaches the scaling of $t^{1/4}$. All curves are obtained for $\gamma = 0.3 \hbar/[m \Delta z^2(0)]$. The arrows mark the points in time shown in Fig. 3

We are now in the position to discuss the time dependence of the frequency ω of the harmonic oscillator shown in Fig. 2b, and find from the approximate expression, Eq. (91), for Δz and the definition, Eq. (85), of ω the formula

$$\omega(t) \cong \frac{\hbar}{m \Delta z(0)} \sqrt{\frac{\gamma t}{\Delta z^2(0) + \frac{\hbar^2}{m^2} t^2}} \tag{95}$$

which for

$$t \ll \frac{m \Delta z^2(0)}{\hbar} \quad (96)$$

increases as $t^{1/2}$, that is

$$\omega(t) \cong \frac{\hbar}{m \Delta z^2(0)} \sqrt{\gamma t}, \quad (97)$$

but eventually decreases as $t^{-1/2}$, that is

$$\omega(t) \cong \sqrt{\frac{\gamma}{t}}. \quad (98)$$

However, from the asymptotic formula, Eq. (94), of Δz valid for $1 \ll \gamma t$ we obtain the correct decay

$$\omega(t) \cong \frac{1}{2} \sqrt{\frac{\gamma}{t}}, \quad (99)$$

which is half of the large-time limit, Eq. (98), of Eq. (95).

In Fig. 2b we compare and contrast the numerically obtained frequency with the approximate but analytical expressions, Eqs. (95) and (99), and find excellent agreement.

5.2.2 Wave Packet

Finally, we exemplify in Fig. 3 the time dependence of the probability density $|\psi(z, t)|^2$ and the corresponding potential $V = V(z, t)$ for four characteristic moments in time. The four images represent four *non-equidistant* points in time to account for the exponential deceleration of the wave packet.

We start in Fig. 3a from $t = 0$ with the initial probability density and the associated linear potential. At this time the quadratic potential vanishes since $\omega(t = 0) = 0$.

In the three subsequent sub-figures (b), (c), and (d) the potential which is co-moving with the particle is always the sum of a linear and a quadratic part corresponding to a displaced harmonic oscillator. The steepness of the linear part is exponentially damped since it is proportional to $\bar{v}(t)$. In contrast, the prefactor of the harmonic part first increases from zero before it decreases again.

5.3 Dynamics in Phase Space

We conclude this section by depicting the time evolution of the Gaussian wave packet in *phase space*. Indeed, often quantum phenomena become rather intuitive when considered in the framework of the Wigner distribution [1]

$$W(z, p; t) \equiv \frac{1}{2\pi\hbar} \int_{-\infty}^{\infty} dy e^{-ipy/\hbar} \psi^*\left(z - \frac{1}{2}y, t\right) \psi\left(z + \frac{1}{2}y, t\right) \quad (100)$$

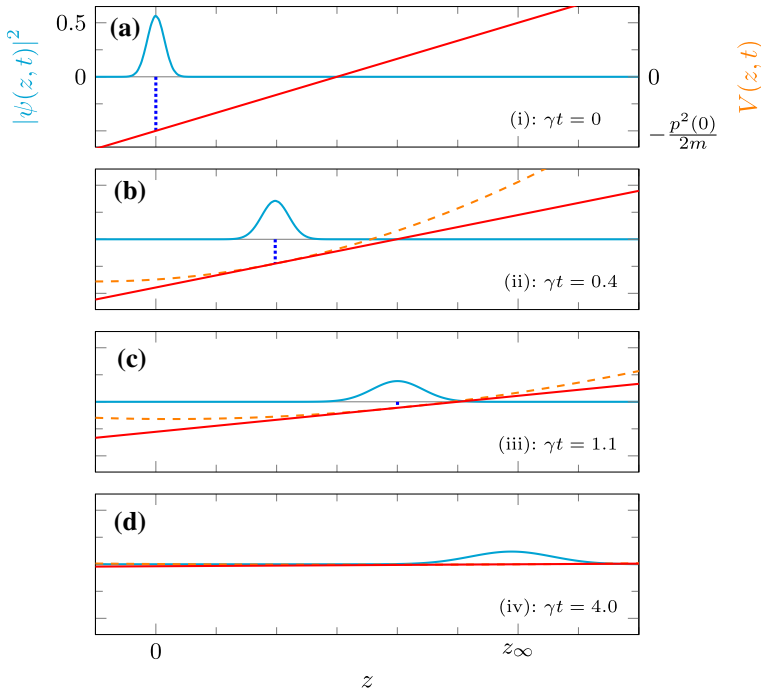


Fig. 3 Time evolution of the Gaussian wave packet, Eq. (42), according to the linear Schrödinger equation, Eq. (47), with the time-dependent potential V defined by Eq. (84), represented by the four non-equidistant points in time indicated by the four arrows in Fig. 2. The probability density $|\psi|^2$ and V are shown by the solid cyan and dashed orange curves, respectively. The linear part of V , Eq. (16), and its off-set determined by the negative kinetic energy are depicted by red tangents and blue dotted vertical lines, respectively. For $t = 0$ the potential V is strictly linear (a) whereas for $t > 0$ it is the sum of a linear and a quadratic term which are both co-moving with the center $\bar{z}(t)$ of the Gaussian. The slope of the linear potential is proportional to \bar{v} and therefore exponentially damped as indicated in (b–d). In contrast, the prefactor of the quadratic part governed by $\omega^2(t)$ first increases from zero and later decreases again. The width of the wave packet displayed in Fig. 2c increases from (a) to (d). The parameters of the initial wave packet are $z(0) = 0$, $\Delta z(0) = z_\infty/30$, and $p(0) = 9\hbar/\Delta z(0)$, and the friction constant is $\gamma = 0.3\hbar/[m\Delta z^2(0)]$

corresponding to the wave function $\psi = \psi(z, t)$. Here the c-numbers z and p play the role of classical phase space variables.

We first analyze the time evolution of the Wigner function and then turn to a discussion of its characteristic features.

5.3.1 Wigner Function

When we substitute the time-dependent Gaussian wave function, Eq. (89) with Eqs. (70) and (90), into the definition, Eq. (100), of the Wigner function and perform the integrations, we obtain the two-dimensional Gaussian function

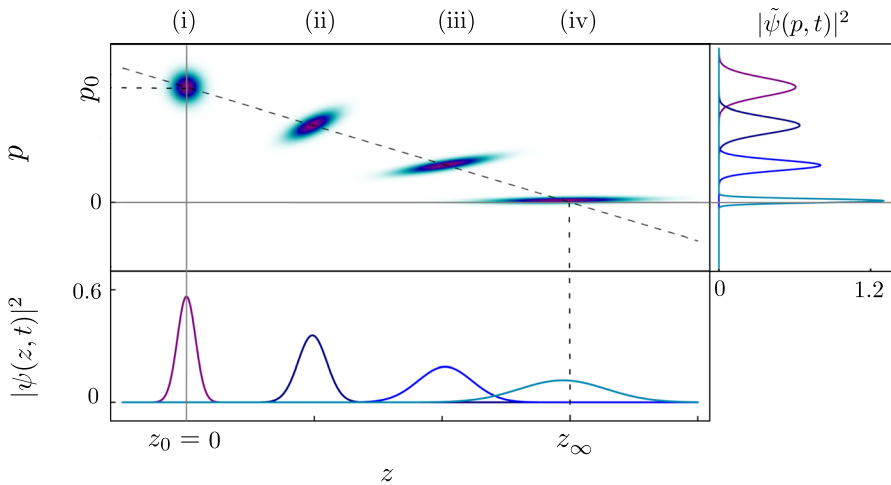


Fig. 4 Phase space dynamics of the Wigner function (main frame) corresponding to the decelerating Gaussian wave packet, Eq. (89), and marginal distributions (bottom and right side). The center of the Gaussian phase space distribution, depicted here for the four times displayed also in Figs. 2 and 3 follows the classical trajectory, Eq. (30), that is the straight line connecting the points $(z_0 = 0, p_0)$ and $(z_\infty, p = 0)$ of slope γ . In appropriate phase space variables, the initial Wigner function is symmetric in z and p , but gets squeezed and misaligned with respect to the axes of phase space as time increases. In the asymptotic limit $t \rightarrow \infty$, it approaches a distribution which is perfectly aligned with the position axis and has a vanishing mean momentum. At the bottom and on the right side of the main frame we show the marginals of the four distributions, that is the corresponding probability densities $|\psi(z, t)|^2$ and $|\tilde{\psi}(p, t)|^2$ in position and momentum. Whereas the position distribution widens, the one in momentum gets infinitely narrow

$$\begin{aligned}
 W(z, p; t) = & \frac{1}{\pi \hbar} \exp \left\{ - \left[\frac{z - \bar{z}(t)}{\delta z(t)} \right]^2 \right\} \exp \left\{ - \left[\frac{p - m\bar{v}(t)}{\hbar / \Delta z(t)} \right]^2 \right\} \\
 & \times \exp \left\{ 2\kappa(t)[z - \bar{z}(t)][p - m\bar{v}(t)] / \hbar \right\}, \tag{101}
 \end{aligned}$$

where the width

$$\delta z(t) \equiv \frac{\Delta z(t)}{\sqrt{1 + \kappa^2(t)}} \tag{102}$$

in position is modified by the square root containing the expression

$$\kappa(t) \equiv \frac{m}{\hbar} \Delta z(t) \frac{d}{dt} \Delta z(t). \tag{103}$$

In the center of Fig. 4 we display $W = W(z, p; t)$, given by Eq. (101), for the characteristic times of Fig. 3 and note three features: (i) The center of W moves along the straight classical phase space trajectory given by Eq. (30). (ii) The Gaussian gets

squeezed in one direction at the expense of the other, and (iii) the major and minor axes of the Gaussian get first misaligned with respect to the axes of phase space but eventually realign. The last effect is due to the cross term between position and momentum of strength $2\kappa(t)$ in the Wigner function, Eq. (101).

Moreover, with the help of the marginals

$$\int_{-\infty}^{\infty} dp W(z, p; t) = |\psi(z, t)|^2 \quad (104)$$

and

$$\int_{-\infty}^{\infty} dz W(z, p; t) = |\tilde{\psi}(p, t)|^2, \quad (105)$$

we obtain the probability densities $|\psi(z, t)|^2$ in position, and $|\tilde{\psi}(p, t)|^2$ in momentum, by integration of the Wigner function over the conjugate variable, where $\tilde{\psi}$ is the Fourier transform of ψ .

As a consequence, we find from Eq. (101) by integration over momentum the Gaussian, Eq. (70), in position space, and by integration over position the Gaussian momentum distribution

$$|\tilde{\psi}(p, t)|^2 = \frac{1}{\sqrt{\pi} \Delta p(t)} \exp \left\{ - \left[\frac{p - m\bar{v}(t)}{\Delta p(t)} \right]^2 \right\} \quad (106)$$

with

$$\Delta p(t) \equiv \frac{\hbar}{\Delta z(t)} \sqrt{1 + \kappa^2(t)}. \quad (107)$$

The time evolution of the probability densities $|\psi(z, t)|^2$ and $|\tilde{\psi}(p, t)|^2$ is displayed in the bottom and the right panel of Fig. 4, respectively. For increasing time t , the probability density in position becomes wider while the center of the Gaussian approaches asymptotically the position z_∞ . At the same time, the probability density in momentum gets sharper, and its center tends toward the momentum $p = 0$. Consequently, for large times t we obtain approximately a momentum eigenstate with vanishing eigenvalue.

5.3.2 Squeezing and Rotation

In order to gain deeper insight into the dynamics of the Wigner function, we now analyze several characteristic features. First, we focus on the time dependence of the width Δz in position, determined by the Pinney equation, Eq. (86), and the width Δp in momentum, Eq. (107), shown in Fig. 5a by magenta and light blue lines, respectively. In agreement with Fig. 4, the width in position increases while the width in momentum decreases as a function of time t .

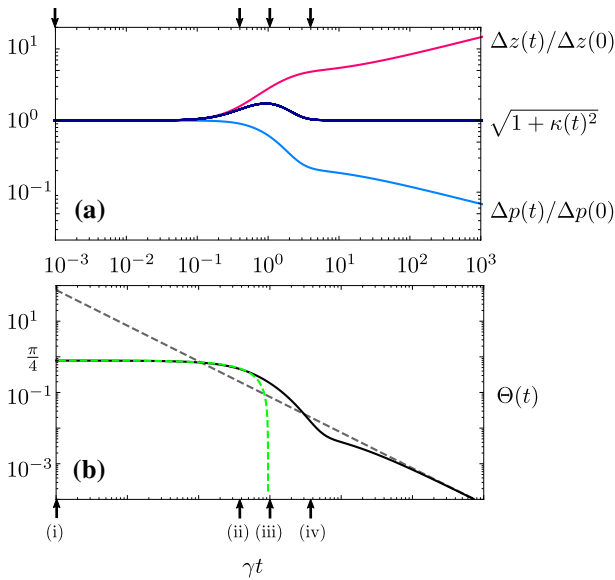


Fig. 5 Time evolution of characteristic features of the Wigner function $W = W(z, p; t)$, given by Eq. (101), such as (a) the dimensionless widths $\Delta z(t)/\Delta z(0)$ and $\Delta p(t)/\Delta p(0)$ in position (magenta) and momentum (light blue), and (b) the rotation angle $\Theta = \Theta(t)$. The arrows mark the characteristic times of Figs. 2, 3 and 4. According to Eq. (107), the product of both quantities is proportional to $\sqrt{1 + \kappa^2(t)}$ (dark blue). While the width in position increases, the width in momentum decreases, leading to an asymptotically constant value of their product for large times t . (b) The rotation angle $\Theta = \Theta(t)$, Eq. (108), shown by the solid black line defines the orientation of the Wigner function in phase space. As a function of the dimensionless time γt it decays from $\pi/4$ to zero. The short and long-time limits of Θ , given by Eqs. (110) and (111), are depicted by the dashed green and dashed gray lines, respectively

Moreover, we note that their product $\Delta z(t)\Delta p(t)/\hbar$, given according to Eq. (107) by $\sqrt{1 + \kappa^2(t)}$, is approximately constant for both small and large times t as depicted by the dark blue line in Fig. 5a. In the intermediate regime with $\gamma t \cong 1$, the function $\sqrt{1 + \kappa^2(t)}$ first increases in time, reaches a maximum and then decays. This is due to the different short- and long-time behaviours of $\kappa \sim t$ and $\kappa \sim t^{-1/2}$ derived in Appendix 2.

Next, we focus on the orientation of the Wigner function W defined by Eq. (101) in phase space. For this purpose, we recall in Appendix 2 the rotation angle

$$\Theta(t) = \frac{1}{2} \arctan \left(\frac{2\kappa(t)\sigma^2(t)}{\sigma^4(t) - [1 + \kappa^2(t)]} \right) \tag{108}$$

of a squeezed coherent state [45] determined by the function $\kappa = \kappa(t)$, Eq. (103), and the scaled width

$$\sigma(t) \equiv \frac{\Delta z(t)}{\Delta z(0)}. \quad (109)$$

In Fig. 5b we display the numerically determined time dependence of Θ , Eq. (108), by a black solid line. In Appendix 2, we also derive the approximate expressions

$$\Theta(t) \cong \frac{\pi}{4} - \frac{\hbar t}{4m\Delta z^2(0)} \quad (110)$$

and

$$\Theta(t) \cong \frac{m}{4\hbar t} \Delta z^2(0) \quad (111)$$

valid in the short and long-time limit, and represented in Fig. 5b by a dashed green and a dashed gray line, respectively. Both approximations are in excellent agreement with the exact numerical result for $\Theta = \Theta(t)$ in their respective domains of validity.

In the limit $t \rightarrow 0$, the rotation angle Θ approaches the value $\pi/4$, whereas for $t \rightarrow \infty$, the angle Θ tends toward zero, corresponding to a perfect alignment of the Wigner function with the position axis of phase space. This result confirms our observation that due to the Schrödinger time evolution in the potential V , given by Eq. (84), we arrive for large times t at an approximate momentum eigenstate of vanishing eigenvalue.

6 Toward an Experimental Implementation

Motivated by the nonlinear Kostin equation we have analyzed in the preceding sections in great detail several ways to decelerate a quantum particle using appropriately designed forces. One technique stands out most clearly due to its simplicity. We expose the wave packet to a parabolic barrier³ whose height is identical to the macroscopic kinetic energy. As a result, the particle approaches in an exponential time an approximate momentum eigenstate of vanishing eigenvalue.

In the present section, we briefly address two ways to implement this approach in an experiment. Our first technique takes advantage of the analogy [47] between the wave equation of surface gravity water waves and the Schrödinger equation. The second idea employs cold atoms stored in a trap provided by an atom chip.

Throughout this section, we try to convey concepts rather than details. In the language of John Archibald Wheeler we are proposing “ideas for ideas”. Nevertheless, we emphasize that first steps toward implementations have already been taken, and more details will be reported in future publications.

³ We note that the model of a parabolic barrier and the associated redistribution of fluctuations also appears in the field of cosmology [46].

6.1 Surface Gravity Water Waves

A unique system to test predictions of the Schrödinger equation consists of surface gravity water waves. Under appropriate conditions the evolution of their surface elevation satisfies [47] a Schrödinger equation in which time and position are interchanged. Moreover, it is also possible to implement external potentials such as a linear or a quadratic one and prepare wave packets with a nonvanishing momentum [48].

The laboratory of Lev Shemer at Tel Aviv University operates several water tanks where numerous experiments of this type have been performed. Rather than going into the detail we refer to the literature but emphasize that in this way it was, for example, possible to measure for the first time the Kennard phase [49, 50], periodic wave trains in nonlinear media [51], or study Bohmian mechanics of macroscopic waves [52].

In connection with the observation [53] of the logarithmic phase singularity [54] which is at the very heart of the Hawking-Unruh radiation [55], Georgi Gary Rozenman has performed [56, 57] a series of experiments in which Gaussian wave packets have come to a rest at the top of a parabolic barrier. He has noticed that at this point the wave disappears, that is the amplitude is too small to be measured. This feature might well be an indication that the wave packet is spread “everywhere” as suggested by a momentum eigenstate.

We emphasize again that the results of G.G. Rozenman are preliminary but his experiments will be continued and analyzed theoretically. They represent a valuable step in the right direction.

6.2 Cold Atoms

In our second implementation we take advantage of the well-established techniques of cold atoms in a chip trap. We emphasize that this technology is now routinely employed even in space [58, 59] and can easily be adjusted to the present problem.

Indeed, we envision a Bose-Einstein condensate (BEC) of ^{87}Rb -atoms in a state $|F = 2, m_F = +2\rangle$ stored in a magnetic trap. We create the macroscopic velocity analogous to the beam by a kick of the trap and then switching it off except the bias field.

Next, we apply a microwave signal to transfer the atoms to the anti-binding state $|F = 2, m_F = -2\rangle$ and turn on again the trap. As a result, the BEC now climbs up a parabolic barrier. The currents on the trap allow us to adjust the initial kick, that is the initial velocity, as well as the initial center-of-mass position of the BEC relative to the location of the maximum of the inverted oscillator.

7 Summary and Conclusions

In quantum theory, the potential determines, with the help of the time-independent Schrödinger equation subjected to appropriate boundary conditions, uniquely the energy spectrum. However, the inverse is not true. Many different potentials can give rise to the same energy spectrum.

In the present article, we have noted a similar violation of uniqueness in the context of a dissipative force. The resulting exponential damping of the velocity and the associated trajectory can also be caused by many different non-dissipative forces. However, there is a subtlety. These mock-up forces depend on the parameters of the desired damped motion such as the initial coordinate and the initial velocity. Hence, the motion is determined by itself and we are facing a nonlinear problem despite the fact that the corresponding Newton equation of motion is still linear.

This approach of decelerating a particle with the help of a time-dependent homogeneous force, or a time-independent inverted harmonic oscillator, works well for a single particle provided the initial conditions are known. However, it cannot be applied to an ensemble of particles of different initial conditions since one single force cannot direct all particles.

On first sight this observation seems to negate the possibility of transferring this technique to quantum mechanics. However, in the present article we have found for a Gaussian wave packet that the same potentials which decelerate the classical particle also force the Gaussian wave packet to follow with its center the classical damped trajectory. In addition, the time dependence of the width of the wave packet determines the final quantum state.

For decelerating Gaussians there is a close connection between the potential creating the motion and the phase of the wave function. For a particular choice of the time-dependence of the width and the off-set of the potential we find that the resulting Schrödinger equation is nonlinear and the potential is proportional to the phase. A particular example of such a nonlinear Schrödinger equation is the Kostin equation.

We have studied the dynamics predicted by a Kostin-like equation in position as well as phase space, and have identified the origin of the exponential deceleration. Indeed, the motion takes place in a time-dependent linear potential moving with the particle, and tracing out a time-independent inverted harmonic oscillator in the laboratory frame. Hence, the wave packet starts on the separatrix in phase space and follows it toward the origin. At the same time, it gets squeezed and rotated approximating in the asymptotic limit of infinite time a momentum eigenstate of vanishing eigenvalue.

We emphasize that the method pursued in this article is more general and can be employed to create a rather general class of final quantum states. In this way, the Kostin approach toward damping of using a nonlinear Schrödinger equation with a potential governed by the phase of the wave function, and the associated techniques to create by time-dependent fields a quantum state of a decelerated particle, are intimately connected to the theme of coherent control.

We admit that in our article we have only given a flavor of this approach of decelerating a quantum particle and have not addressed many issues that come to mind: (i) Can this method be generalized to initial wave functions other than Gaussians? (ii) How sensitive is the dependence of the potential on the parameters of the initial state? and (iii) What is the cost function that makes the Kostin potential optimal?

Although we cannot provide definite answers to these questions at the moment, we are confident that we will have them for the next round birthday of David and John. Again our warmest wishes and Happy Birthday!

Appendix 1: Derivation of Potentials

In this appendix we search for a potential which causes a Gaussian wave packet to slow down exponentially due to the Schrödinger dynamics. We show that the potential that achieves this goal is not unique but depends on the desired time evolution of the width of the wave packet.

Moreover, a closer examination of our calculation reveals that at no point the specific form of the center-of-mass motion enters. As a result, our technique allows us to find the potential giving rise to the probability density following *any* predetermined classical trajectory of the particle. In particular, we can not only exponentially decelerate but also accelerate it.

Our derivation relies on a mathematical identity [8] which constitutes the backbone of the Schrödinger equation, and we pursue as follows: The continuity equation for the Gaussian probability density provides us with the phase of the wave function. Moreover, together with the so-obtained phase and the required motion of the probability density, the quantum Hamilton-Jacobi equation governs, for a given time dependence of the width, the potential.

It is at this point that the non-uniqueness emerges. Indeed, a different choice of the dynamics of the width yields a different potential.

Outline of the Calculation

Throughout this appendix we focus exclusively on the dynamics of the Gaussian wave packet

$$\psi(z, t = 0) \equiv \frac{1}{\sqrt[4]{\pi}} \frac{1}{\sqrt{\Delta z(0)}} \exp \left\{ -\frac{1}{2} \left[\frac{z - \bar{z}(0)}{\Delta z(0)} \right]^2 \right\} \exp \left\{ \frac{i}{\hbar} m v(0) [z - \bar{z}(0)] \right\} \quad (112)$$

and search for a potential V for which the Schrödinger equation

$$i\hbar \frac{\partial}{\partial t} \psi + \frac{\hbar^2}{2m} \frac{\partial^2}{\partial z^2} \psi = V\psi \quad (113)$$

leads us to the probability density

$$W(z, t) \equiv |\psi(z, t)|^2 \equiv \frac{1}{\sqrt{\pi}} \frac{1}{\Delta z(t)} \exp \left\{ -\left[\frac{z - \bar{z}(t)}{\Delta z(t)} \right]^2 \right\} \equiv A^2, \quad (114)$$

where $\bar{z} = \bar{z}(t)$ is determined by the classical trajectory.

Although we have the exponentially decelerated trajectory, Eq. (6), in mind, we emphasize that the specific form of $\bar{z} = \bar{z}(t)$ is not relevant to our calculation. Hence, we can find in this way the potential giving rise to any prescribed motion of the center of the Gaussian probability density W . Moreover, we show that this requirement does not determine the time-dependent width $\Delta z = \Delta z(t)$ of the Gaussian wave packet.

Our analysis relies on the mathematical identity [8]

$$i \frac{\partial}{\partial t} \mathcal{Z} + \beta \frac{\partial^2}{\partial z^2} \mathcal{Z} = \left[\mathcal{V} + i \frac{1}{2A^2} \mathcal{C} \right] \mathcal{Z} \quad (115)$$

for the complex valued function

$$\mathcal{Z} = \mathcal{Z}(z, t) \equiv A(z, t) e^{i\theta(z, t)} \quad (116)$$

where

$$\mathcal{V} \equiv -\frac{\partial}{\partial t} \theta - \beta \left(\frac{\partial}{\partial z} \theta \right)^2 + \beta \frac{1}{A} \frac{\partial^2}{\partial z^2} A \quad (117)$$

and

$$\mathcal{C} \equiv \frac{\partial}{\partial t} A^2 + 2\beta \frac{\partial}{\partial z} \left(A^2 \frac{\partial}{\partial z} \theta \right). \quad (118)$$

Here β is a constant as to match the units of the two derivatives on the left-hand side of Eq. (115).

From a comparison between Eqs. (113) and (115) we note that three requirements transform this mathematical identity into the Schrödinger equation: (i) multiplication by \hbar , (ii) the choice $\hbar/(2m)$ for β , and (iii) conservation of probability, that is $\mathcal{C} = 0$. In this case the desired potential reads $V \equiv \hbar \mathcal{V}$.

Hence, we pursue in three steps: (i) We first substitute the probability density W into Eq. (118), and find with $\mathcal{C} = 0$ the associated phase θ . (ii) We adjust θ to the initial conditions of ψ at $t = 0$ which fixes β , and (iii) substitute θ into the analogue of the Hamilton-Jacobi equation, Eq. (117), to obtain V .

Phase from Continuity Equation

We start by evaluating the derivatives of W given by Eq. (114) with respect to time and space in the expression

$$\mathcal{C} = \frac{\partial}{\partial t} W + 2\beta \left(\frac{\partial}{\partial z} W \right) \frac{\partial}{\partial z} \theta + 2\beta W \frac{\partial^2}{\partial z^2} \theta, \quad (119)$$

following from Eq. (118).

Conservation of probability, that is

$$\mathcal{C} = 0, \quad (120)$$

leads us to the partial differential equation

$$0 = -\frac{1}{\Delta z} \left(\frac{d}{dt} \Delta z \right) + 2 \frac{z - \bar{z}}{\Delta z^2} \bar{v} + 2 \frac{(z - \bar{z})^2}{\Delta z^3} \left(\frac{d}{dt} \Delta z \right) - 4\beta \frac{z - \bar{z}}{\Delta z^2} \frac{\partial}{\partial z} \theta + 2\beta \frac{\partial^2}{\partial z^2} \theta \quad (121)$$

of second order for θ .

It is straightforward to verify by substitution into Eq. (121) that the function

$$\theta(z, t) \equiv \frac{1}{4\beta} \frac{1}{\Delta z} \left(\frac{d}{dt} \Delta z \right) (z - \bar{z})^2 + \frac{1}{2\beta} \bar{v} (z - \bar{z}) + f(t), \quad (122)$$

where the time-dependent function $f = f(t)$ is independent of z , is indeed a solution.

A comparison with the initial wave function, Eq. (112), yields the initial conditions

$$\left. \frac{d}{dt} \Delta z(t) \right|_{t=0} = 0 \quad (123)$$

and

$$f(0) = 0 \quad (124)$$

as well as the choice

$$\beta \equiv \frac{\hbar}{2m} \quad (125)$$

for the constant β .

Hence, we arrive at the expression

$$\theta = \frac{1}{\hbar} S \equiv \frac{1}{\hbar} \left\{ \frac{m}{2} \frac{1}{\Delta z} \left(\frac{d}{dt} \Delta z \right) (z - \bar{z})^2 + m \bar{v} (z - \bar{z}) + s(t) \right\} \quad (126)$$

for the phase θ where we have introduced the abbreviation

$$s(t) \equiv \hbar f(t), \quad (127)$$

which due to Eq. (124), enjoys the initial condition

$$s(0) = 0. \quad (128)$$

Hence, θ involves the coordinate z in a linear and a quadratic way, always relative to the classical motion $\bar{z} = \bar{z}(t)$. Moreover, the strength of the quadratic contribution is governed by the time dependence of the width whereas the one of the linear term is determined by the classical velocity $\bar{v} = \bar{v}(t)$. In addition there is a purely time-dependent function $s = s(t)$ which will allow us to achieve a proportionality between θ and V , and arrive at the Kostin equation.

Potential

We are now in the position to determine the potential. For this purpose, we substitute the expression, Eq. (126), for θ together with Eq. (114) for W into the definition, Eq. (117), of \mathcal{V} and arrive at the expression

$$V \equiv \hbar \mathcal{V} \equiv -\frac{m}{2} \frac{1}{\Delta z} \left[\left(\frac{d^2}{dt^2} \Delta z \right) - \frac{\hbar^2}{m^2} \frac{1}{\Delta z^3} \right] (z - \bar{z})^2 - m \left(\frac{d}{dt} \bar{v} \right) (z - \bar{z}) + \frac{m}{2} \bar{v}^2 - \frac{d}{dt} s - \frac{\hbar^2}{2m} \frac{1}{\Delta z^2}, \quad (129)$$

where we have used Eq. (5) to replace the time derivative of \bar{z} by \bar{v} .

Hence, V contains terms quadratic and linear in the coordinate z as well as purely time-dependent functions. Moreover, these contributions are always relative to the classical trajectory $\bar{z} = \bar{z}(t)$. It is remarkable that the explicit form of \bar{z} , given for deceleration by Eq. (6), has not entered into the derivation. As a result, the potential defined by Eq. (129) is valid for any desired motion $\bar{z} = \bar{z}(t)$.

We emphasize that apart from the trajectory also the acceleration of the particle appears in the linear deviation from \bar{z} , and that there still exists a lot of freedom in the choice of V . Indeed, the Schrödinger equation does not specify s nor Δz . They depend on the desired final state of the motion as explained in Sect. 3.

We conclude by reducing the potential of Eq. (129) to the one causing an exponential deceleration of the probability density. For this purpose, we recall Eq. (2) to replace the time derivative of \bar{v} by $-\gamma \bar{v}$ and arrive at

$$V \equiv \hbar \mathcal{V} \equiv -\frac{m}{2} \frac{1}{\Delta z} \left[\left(\frac{d^2}{dt^2} \Delta z \right) - \frac{\hbar^2}{m^2} \frac{1}{\Delta z^3} \right] (z - \bar{z})^2 + \gamma m \bar{v} (z - \bar{z}) + \frac{m}{2} \bar{v}^2 - \frac{d}{dt} s - \frac{\hbar^2}{2m} \frac{1}{\Delta z^2}, \quad (130)$$

where now the trajectory $\bar{z} = \bar{z}(t)$ is not arbitrary anymore but given by Eq. (6).

Appendix 2: Rotated Wigner Distribution

Figure 4 shows that the propagation of the Gaussian wave packet in Wigner phase space is accompanied by a rotation. In this appendix we first derive an expression for the angle Θ between the coordinate axis and the major axis of the rotated Gaussian Wigner distribution, and then apply these results to the Kostin dynamics presented in Sect. 5.3, that is we analyze the dynamics of Θ enforced by the time dependence of Δz due to the Pinney equation. We conclude by discussing the short- and long-time limits of this expression and find approximate but analytical expressions.

Determination of Rotation Angle

We start from a non-diagonal Wigner function

$$W(Z, P) = \frac{1}{\pi} \exp(-aZ^2 - bP^2 + 2cZP) \quad (131)$$

in the phase space spanned by the dimensionless position Z and momentum P with coefficients a , b , and c .

Next we introduce a new set of variables Z' and P' which are connected to Z and P by the rotation

$$\begin{pmatrix} Z \\ P \end{pmatrix} = \begin{pmatrix} \cos \Theta & -\sin \Theta \\ \sin \Theta & \cos \Theta \end{pmatrix} \begin{pmatrix} Z' \\ P' \end{pmatrix}, \quad (132)$$

and choose Θ such that in the new coordinates W is diagonal, that is

$$W(Z', P') = \frac{1}{\pi} \exp(-a'Z'^2 - b'P'^2), \quad (133)$$

with coefficients a' and b' .

Indeed, when we substitute Z and P given by Eq. (132) into the Wigner function, Eq. (131), and combine the cross terms $Z'P'$ arising from Z^2 , P^2 and ZP we arrive at the condition

$$(a - b) \sin(2\Theta) + 2c \cos(2\Theta) = 0, \quad (134)$$

or

$$\Theta = \frac{1}{2} \arctan\left(\frac{2c}{b-a}\right). \quad (135)$$

We now apply this result to the Wigner function

$$\begin{aligned} W(z, p) &= \frac{1}{\pi \hbar} \exp\left[-\left(\frac{z - \bar{z}}{\delta z}\right)^2\right] \exp\left[-\left(\frac{p - m\bar{v}}{\hbar/\Delta z}\right)^2\right] \\ &\times \exp\left[2\kappa(z - \bar{z})(p - m\bar{v})/\hbar\right] \end{aligned} \quad (136)$$

obtained in Sect. 5.2 with

$$\delta z \equiv \frac{\Delta z}{\sqrt{1 + \kappa^2}}. \quad (137)$$

Since the phase space variables (Z, P) as well as (Z', P') are dimensionless we first introduce the new set of coordinates

$$Z \equiv \frac{z - \bar{z}}{\Delta z(0)} \quad (138)$$

and

$$P \equiv \frac{p - m\bar{v}}{\hbar/\Delta z(0)} \quad (139)$$

together with the scaled width

$$\sigma \equiv \frac{\Delta z}{\Delta z(0)}. \quad (140)$$

In this variables the phase space distribution, Eq. (136), takes the form

$$W(Z, P) = \frac{1}{\pi} \exp\left(-\frac{1 + \kappa^2}{\sigma^2} Z^2 - \sigma^2 P^2 + 2\kappa ZP\right). \quad (141)$$

A comparison between Eqs. (131) and (141) yields the identifications $a \equiv (1 + \kappa^2)/\sigma^2$, $b \equiv \sigma^2$, and $c \equiv \kappa$ which together with the formula Eq. (135) for Θ provides us with the expression

$$\Theta = \frac{1}{2} \arctan\left[\frac{2\kappa\sigma^2}{\sigma^4 - (1 + \kappa^2)}\right] \quad (142)$$

for the rotation angle.

From the definition, Eq. (140), of σ and

$$\kappa(t) \equiv \frac{m}{\hbar} \Delta z(t) \frac{d}{dt} \Delta z(t), \quad (143)$$

we note that the time dependence of $\Theta = \Theta(t)$ is solely determined by that of the width $\Delta z = \Delta z(t)$ following from the Pinney equation, Eq. (86).

Dynamics

In the preceding section, we have derived an expression for the rotation angle Θ in terms of the two parameters σ and κ of the Gaussian Wigner function corresponding to the Gaussian wave packet decelerated by the Kostin dynamics. We now consider Θ in the short and long-time limit.

For short times we recall from Eq. (91) the approximation

$$\Delta z(t) \cong \left[\Delta z^2(0) + \frac{\hbar^2}{m^2} \frac{t^2}{\Delta z^2(0)} \right]^{\frac{1}{2}}, \quad (144)$$

which for $t \rightarrow 0$ leads us to

$$\sigma^4 \cong 1 + 2 \frac{\hbar^2}{m^2} \frac{t^2}{\Delta z^4(0)} \quad (145)$$

where we have used the definition, Eq. (140), of σ .

Moreover, Eq. (144) yields the expression

$$\frac{d}{dt}\Delta z \cong \frac{\hbar^2}{m^2} \frac{t}{\Delta z^3(0)}, \quad (146)$$

and with the definition, Eq. (143), of κ we arrive at

$$\kappa(t) \cong \frac{\hbar}{m} \frac{t}{\Delta z^2(0)}. \quad (147)$$

Hence, Eq. (145) takes the form

$$\sigma^4 \cong 1 + 2\kappa^2. \quad (148)$$

When we substitute this approximation for σ^4 into the expression Eq. (142) for Θ we obtain with $\kappa\sigma^2 \cong \kappa$ the formula

$$\Theta \cong \frac{1}{2} \arctan\left(\frac{2}{\kappa}\right) \quad (149)$$

or

$$\Theta(t) \cong \frac{1}{2} \arctan\left[\frac{2m}{\hbar t} \Delta z^2(0)\right], \quad (150)$$

where we have recalled the explicit form, Eq. (147), of κ .

Finally, the asymptotic expansion

$$\arctan \alpha \cong \frac{\pi}{2} - \frac{1}{\alpha} \quad (151)$$

for $1 \ll \alpha$ leads us to

$$\Theta(t) \cong \frac{\pi}{4} - \frac{\hbar t}{4m\Delta z^2(0)}. \quad (152)$$

Hence, in the short-time limit Θ decreases linearly in t starting from $\pi/4$. In the following appendix we rederive this result from the familiar time evolution of a free particle in phase space and, in particular, shine some light on the starting angle $\pi/4$.

In the long-time limit we employ the approximation Eq. (94), that is

$$\Delta z(t) \cong \sqrt{\frac{2\hbar}{\sqrt{\gamma}m}} t^{\frac{1}{4}} \quad (153)$$

which yields

$$\frac{d}{dt}\Delta z = \frac{1}{4} \sqrt{\frac{2\hbar}{\sqrt{\gamma}m}} t^{-\frac{3}{4}}, \quad (154)$$

and thus

$$\kappa(t) \cong \frac{1}{2} \frac{1}{\sqrt{\gamma}} t^{-\frac{1}{2}}. \quad (155)$$

Since for $t \rightarrow \infty$ we find from Eqs. (153) and (155) the behaviors $\sigma^4 \sim t$ and $\kappa \sim t^{-1/2}$ we can neglect in the expression, Eq. (142), for Θ the contribution $1 + \kappa^2 \sim 1 + t^{-1}$ compared to σ^4 , and arrive at the approximation

$$\Theta \cong \frac{1}{2} \arctan \left(\frac{2\kappa}{\sigma^2} \right), \quad (156)$$

which with Eqs. (153) and (155) reduces to

$$\Theta(t) \cong \frac{1}{2} \arctan \left\{ \frac{m}{2\hbar t} [\Delta z(0)]^2 \right\}, \quad (157)$$

or

$$\Theta(t) \cong \frac{m}{4\hbar t} [\Delta z(0)]^2 \quad (158)$$

where we have used the familiar expansion

$$\arctan \alpha \cong \alpha \quad (159)$$

valid for $\alpha \ll 1$.

Hence, in the limit of $t \rightarrow \infty$ we find $\Theta \rightarrow 0$, that is the Wigner function aligns itself with the z -axis of phase space.

Appendix 3: Rotation Angle for Free Motion

In the preceding appendix we have shown that the time evolution of a symmetric Gaussian Wigner function governed by the Kostin equation involves the squeezing and the rotation of this phase space distribution function. In particular, we have found that the rotation angle decreases starting from $\pi/4$ and eventually approaches zero. Our approach of Appendix 2 has relied on first deriving a general expression for the rotation angle of a non-diagonal Gaussian Wigner function, and then applying this formula to the Kostin dynamics.

Since at least for short times even the Kostin equation predicts a free motion, it is worthwhile to compare and contrast the time evolution of the rotation angle discussed in Appendix 2 to the one of free motion. Here we use two independent but complementary techniques: (i) We first employ the formalism of the first subsection of Appendix 2 to obtain an expression for $\Theta = \Theta(t)$ valid for all values of t , and then obtain the short- and long-time limit, and (ii) we rederive the short-time result by solving a variational problem. For this purpose, we determine at a given time the point on the phase space curve corresponding to a contour line of the Gaussian Wigner function whose separation from the origin assumes a maximum. The point is then the vertex of the ellipse.

For the sake of simplicity we use throughout this appendix the dimensionless phase space variables Z and P of the first subsection of Appendix 2.

The Mystery of the Starting Angle

The reason for our analysis complementing the one of Appendix 2 is that conventional wisdom associates with the starting value of Θ the angle $\pi/2$ rather than $\pi/4$. Indeed, the free time-evolution of every point (Z_0, P_0) in phase space undergoes a translation

$$Z(t) = Z_0 + P_0 t \quad (160)$$

of the coordinate, while the momentum is constant, that is

$$P(t) = P_0. \quad (161)$$

Hence, the point $Z_0 = 0$ and $P_0 = 1$ of a circular contour line

$$P_0^2 + Z_0^2 = 1 \quad (162)$$

of a symmetric Gaussian Wigner function has the largest momentum whereas $Z_0 = 1, P_0 = 0$ or $Z_0 = -1, P_0 = 0$ do not move at all. The concentration on these three points in phase space does indeed suggest that Θ starts from $\pi/2$ rather than $\pi/4$.

However, we gain deeper insight into the dynamics by considering the time evolution of the *complete* circular contour line, Eq. (162), rather than the three points, which by the substitution, Eqs. (160) and (161), develops into the curve

$$P^2 + (Z - Pt)^2 = 1, \quad (163)$$

that is a rotated ellipse

$$Z^2 + (1 + t^2)P^2 - 2tZP = 1, \quad (164)$$

as shown in Fig. 6.

From a comparison between Eq. (164) and the definition, Eq. (131), of the Gaussian phase space distribution function we can read off the coefficients $a = 1$, $b = 1 + t^2$ and $c = t$, and find from the expression, Eq. (135), for the rotation angle Θ the formula

$$\Theta = \frac{1}{2} \arctan\left(\frac{2}{t}\right), \quad (165)$$

which for $t \rightarrow 0$ takes the form

$$\Theta \cong \frac{\pi}{4} - \frac{t}{4}. \quad (166)$$

Here we have used the expansion, Eq. (151).

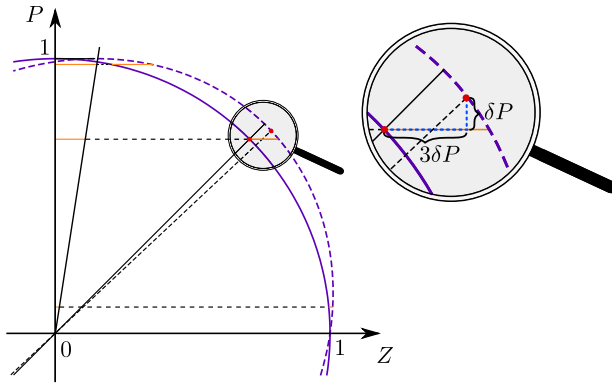


Fig. 6 Phase space explanation of the formation of an ellipse due to free time-evolution from the initial circle with its major axis emerging from the diagonal of this quadrant, that is the angle $\pi/4$. Every point of the circle of radius unity gets shifted during the time t by an amount Pt proportional to the momentum P as indicated by the inclined line. Points with $P \lesssim 1$ reach a larger value of Z than the one with $P = 1$ due to the sharp increase of the initial coordinate as P decreases starting from $P = 1$. This behavior causes a symmetry breaking with respect to the diagonal. In a time t the vertex of the ellipse moves up in its momentum from the diagonal by an amount $\delta P = t/4\sqrt{2}$ but in its position three times as much to the right as shown in the magnifying glass. As a result, the rotation angle decreases with increasing t starting from $\pi/4$

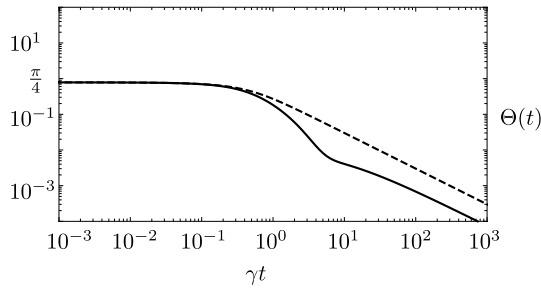


Fig. 7 Comparison between the time evolutions of the rotation angle Θ of the ellipse formed by the contour lines of the Gaussian Wigner function governed by the Kostin dynamics (solid line) and the free particle (dashed curve). The short- and long-time limits have the same scalings but the numerical factors are different for $t \rightarrow \infty$. Between the two extreme regions the two curves differ since in this domain of time the quadratic part of the potential, Eq. (84), governs the dynamics

Hence, the starting angle is indeed $\pi/4$, and not $\pi/2$ as suggested by the naive picture.

Moreover, for $t \rightarrow \infty$, the approximation, Eq. (159), of the function \arctan leads us to the asymptotics

$$\Theta(t) \cong \frac{1}{t}. \tag{167}$$

When we compare and contrast the expressions, Eqs. (166) and (167), representing free motion to the corresponding ones, Eqs. (152) and (158), of the Kostin dynamics, we find identical scalings with t . Moreover, in the short-time limit even the factor $1/4$ is identical. However, the long-time limits differ by a factor $1/4$.

In Fig. 7 we depict the complete time dependence of Θ for the Kostin dynamics and that of a free particle. We note that they are rather similar for short and long times. However, in between they differ substantially.

Determination of Vertex

Next we turn to our variational approach toward finding the rotation angle. For this purpose, we cast Eq. (163) into the form

$$Z = \sqrt{1 - P^2} + Pt, \quad (168)$$

that is, we concentrate for the time being on the first quadrant of phase space with $0 < Z$ and $0 < P$.

Figure 6 shows that we shift every point on the circle of radius unity by an amount Pt which depends linearly on P . Hence, the point on the P -axis experiences the largest shift since there the momentum is largest. For this reason, it is tempting to think that the rotation of the ellipse starts at $\pi/2$.

However, the final coordinate Z given by Eq. (168) does not only depend on the shift but also on the Z -coordinate of the point on the circle as expressed by the square root. In particular, for $P \lesssim 1$ this square root increases rapidly from zero as P decreases starting from $P = 1$. This dramatic initial displacement is the deeper reason why Θ decays from $\pi/4$ rather than $\pi/2$.

In order to bring this feature out most clearly we study the separation

$$s \equiv \sqrt{Z^2 + P^2} \quad (169)$$

of a point on the curve, Eq. (168), from the origin. When s assumes a maximum as a function of P we have found the eccentricity of the ellipse, and thus the major axis. The corresponding values of Z and P then determine the rotation angle.

We find the maximum of s by first substituting Eq. (168) into the expression, Eq. (169), for s and by differentiating the resulting formula

$$s = \sqrt{1 + t(2P\sqrt{1 - P^2} + P^2t)}, \quad (170)$$

with respect to P which yields

$$\frac{ds}{dP} = \frac{t}{s} \left(\frac{1 - 2P^2}{\sqrt{1 - P^2}} + Pt \right). \quad (171)$$

For $t = 0$ we obtain an extremum independent of P which corresponds to the initial circle. However, for $t \neq 0$ the condition for the extremum reads

$$\frac{1 - 2P^2}{\sqrt{1 - P^2}} + Pt = 0. \quad (172)$$

Here it is useful to first consider again the case $t = 0$ which predicts

$$P = \frac{1}{\sqrt{2}}, \quad (173)$$

and together with Eq. (168) provides us with

$$Z = \frac{1}{\sqrt{2}}, \quad (174)$$

that is the crossing point of the circle with the diagonal, leading us already to the angle $\pi/4$.

Next, we consider Eq. (172) for a small but non-vanishing value of t which we include in P by allowing a small correction δP , that is

$$P_{\max} = \frac{1}{\sqrt{2}} + \delta P. \quad (175)$$

When we substitute this ansatz into Eq. (172) we find

$$\delta P = \frac{t}{4\sqrt{2}} \quad (176)$$

where we have neglected terms δP^2 and δPt .

We emphasize that δP is linear in t and positive. Hence, for small values of t the momentum

$$P_{\max} = \frac{1}{\sqrt{2}} \left(1 + \frac{t}{4} \right) \quad (177)$$

of the vertex increases linearly in t starting from $1/\sqrt{2}$.

However, the coordinate Z_{\max} corresponding to P_{\max} given by Eq. (168) also increases, and most importantly three times as much. Indeed, when we substitute P_{\max} given by Eq. (177) into the definition, Eq. (168), of Z we arrive at

$$Z_{\max} \equiv Z(P_{\max}) \cong \frac{1}{\sqrt{2}} \left(\sqrt{1 - \frac{t}{2}} + t \right), \quad (178)$$

or

$$Z_{\max} = \frac{1}{\sqrt{2}} \left(1 + \frac{3}{4}t \right). \quad (179)$$

Hence, with the help of the expressions, Eqs. (177) and (179), for P_{\max} and Z_{\max} the rotation angle

$$\Theta \equiv \arctan\left(\frac{P_{\max}}{Z_{\max}}\right) \quad (180)$$

of the ellipse reads

$$\Theta \cong \arctan\left(1 - \frac{t}{2}\right). \quad (181)$$

Here we have neglected again terms quadratic in t .

Finally, with the Taylor expansion

$$\arctan(1 - x) \cong \arctan(1) - \frac{x}{2} = \frac{\pi}{4} - \frac{x}{2} \quad (182)$$

we find

$$\Theta \cong \frac{\pi}{4} - \frac{t}{4}, \quad (183)$$

in complete agreement with the prediction, Eq. (166).

Summary

We conclude by highlighting the key ingredients of this calculation and identify three central insights: (i) According to Eq. (172) the extremum of s for short times is given by a small deviation from the diagonal of the first quadrant. (ii) Although, the corresponding shift in P is positive, the one in Z is three times as large thereby *reducing* the angle relative to the diagonal. (iii) However, this change in angle is only half of the contribution. The other half results from the asymptotic expansion of the arctan around $\alpha = 1$.

Acknowledgements We thank R. Folman, M. Freyberger, A. Friedrich, N. Gaaloul, E. Giese, F. Narducci, G.G. Rozenman and L. Wörner for many stimulating discussions on this topic, and M.C. Downer and P. Hommelhoff for their help with the references. W.P.S. is grateful to Texas A&M University for a Faculty Fellowship at the Hagler Institute for Advanced Study at the Texas A&M University as well as to the Texas A&M AgriLife Research.

Funding Open Access funding enabled and organized by Projekt DEAL.

Data Availability The datasets generated and analyzed during the current study are available from the corresponding author on reasonable request.

Declarations

Competing interests The authors have no competing interests to declare that are relevant to the content of this article.

Open Access This article is licensed under a Creative Commons Attribution 4.0 International License, which permits use, sharing, adaptation, distribution and reproduction in any medium or format, as long as you give appropriate credit to the original author(s) and the source, provide a link to the Creative Commons licence, and indicate if changes were made. The images or other third party material in this article are included in the article's Creative Commons licence, unless indicated otherwise in a credit line to the material. If material is not included in the article's Creative Commons licence and your intended use is

not permitted by statutory regulation or exceeds the permitted use, you will need to obtain permission directly from the copyright holder. To view a copy of this licence, visit <http://creativecommons.org/licenses/by/4.0/>.

References

1. W.P. Schleich, *Quantum Optics in Phase Space* (Wiley-VCH, Berlin, 2001)
2. G. Kurizki, A.G. Kofman, *Thermodynamics and Control of Open Quantum Systems* (Cambridge University Press, Cambridge, 2022)
3. G.W. Ford, J.T. Lewis, R.F. O'Connell, Quantum Langevin equation. *Phys. Rev. A* **37**(11), 4419–4428 (1988). <https://doi.org/10.1103/PhysRevA.37.4419>
4. H. Carmichael, *An Open Systems Approach to Quantum Optics. Lecture Notes in Physics*, vol. 18 (Springer, Berlin, 1993)
5. Y. Castin, K. Mølmer, Monte Carlo wave-function analysis of 3D optical molasses. *Phys. Rev. Lett.* **74**(19), 3772–3775 (1995). <https://doi.org/10.1103/PhysRevLett.74.3772>
6. M.D. Kostin, On the Schrödinger-Langevin equation. *J. Chem. Phys.* **57**(9), 3589–3591 (1972). <https://doi.org/10.1063/1.1678812>
7. F. Haas, J.M.F. Bassalo, D.G. da Silva, A.B. Nassar, M. Cattani, Time-dependent Gaussian solution for the Kostin equation around classical trajectories. *Int. J. Theor. Phys.* **52**(1), 88–95 (2013). <https://doi.org/10.1007/s10773-012-1302-8>
8. W.P. Schleich, D.M. Greenberger, D.H. Kobe, M.O. Scully, Schrödinger equation revisited. *Proc. Natl. Acad. Sci. USA* **110**(14), 5374–5379 (2013). <https://doi.org/10.1073/pnas.1302475110>
9. A. Shimony, Proposed neutron interferometer test of some nonlinear variants of wave mechanics. *Phys. Rev. A* **20**(2), 394–396 (1979). <https://doi.org/10.1103/PhysRevA.20.394>
10. J.J. Bollinger, D.J. Heinzen, W.M. Itano, S.L. Gilbert, D.J. Wineland, Test of the linearity of quantum mechanics by rf spectroscopy of the $^9\text{Be}^+$ ground state. *Phys. Rev. Lett.* **63**(10), 1031–1034 (1989). <https://doi.org/10.1103/PhysRevLett.63.1031>
11. C.G. Shull, D.K. Atwood, J. Arthur, M.A. Horne, Search for a nonlinear variant of the Schrödinger equation by neutron interferometry. *Phys. Rev. Lett.* **44**(12), 765–768 (1980). <https://doi.org/10.1103/PhysRevLett.44.765>
12. A.J. Leggett, Spin diffusion and spin echoes in liquid ^3He at low temperature. *J. Phys. Condens. Matter* **3**(2), 448–459 (1970). <https://doi.org/10.1088/0022-3719/3/2/027>
13. C.J. Pethick, H. Smith, *Bose-Einstein Condensation in Dilute Gases* (Cambridge University Press, Cambridge, 2008). <https://doi.org/10.1017/CBO9780511802850>
14. I. Bialynicki-Birula, J. Mycielski, Nonlinear wave mechanics. *Ann. Phys. (N. Y.)* **100**(1–2), 62–93 (1976). [https://doi.org/10.1016/0003-4916\(76\)90057-9](https://doi.org/10.1016/0003-4916(76)90057-9)
15. S. Weinberg, Testing quantum mechanics. *Ann. Phys. (N. Y.)* **194**(2), 336–386 (1989). [https://doi.org/10.1016/0003-4916\(89\)90276-5](https://doi.org/10.1016/0003-4916(89)90276-5)
16. C. Brif, R. Chakrabarti, H. Rabitz, Control of quantum phenomena: past, present and future. *New J. Phys.* **12**(7), 075008 (2010). <https://doi.org/10.1088/1367-2630/12/7/075008>
17. N. Bohr, On the theory of the decrease of velocity of moving electrified particles on passing through matter. *Philos. Mag.* **25**(145), 10–31 (1913). <https://doi.org/10.1080/14786440108634305>
18. N. Bohr, The penetration of atomic particles through matter. *Mat. Fys. Medd. Dan. Vid. Selsk.* **18**, 1–144 (1948)
19. J. Lindhard, A. Winthner, Stopping power of electron gas and equipartition rule. *Mat. Fys. Medd. Dan. Vid. Selsk.* **34**(4), 1–22 (1964)
20. P. Sigmond, *Stopping of Heavy Ions—A Theoretical Approach. Springer Tracts in Modern Physics*, vol. 204 (Springer, Heidelberg, 2004)
21. T.W. Hänsch, A.L. Schawlow, Cooling of gases by laser radiation. *Opt. Commun.* **13**(1), 68–69 (1975). [https://doi.org/10.1016/0030-4018\(75\)90159-5](https://doi.org/10.1016/0030-4018(75)90159-5)
22. D.J. Wineland, W.M. Itano, Laser cooling of atoms. *Phys. Rev. A* **20**(4), 1521–1540 (1979). <https://doi.org/10.1103/PhysRevA.20.1521>
23. S. Stenholm, The semiclassical theory of laser cooling. *Rev. Mod. Phys.* **58**(3), 699–739 (1986). <https://doi.org/10.1103/RevModPhys.58.699>

24. C.N. Cohen-Tannoudji, Nobel lecture: manipulating atoms with photons. *Rev. Mod. Phys.* **70**(3), 707–719 (1998). <https://doi.org/10.1103/RevModPhys.70.707>
25. S. van der Meer, Stochastic cooling and the accumulation of antiprotons. *Rev. Mod. Phys.* **57**(3), 689–697 (1985). <https://doi.org/10.1103/RevModPhys.57.689>
26. M.G. Raizen, J. Koga, B. Sundaram, Y. Kishimoto, H. Takuma, T. Tajima, Stochastic cooling of atoms using lasers. *Phys. Rev. A* **58**(6), 4757–4760 (1998). <https://doi.org/10.1103/PhysRevA.58.4757>
27. W. Ketterle, D.E. Pritchard, Atom cooling by time-dependent potentials. *Phys. Rev. A* **46**(7), 4051–4054 (1992). <https://doi.org/10.1103/PhysRevA.46.4051>
28. W.D. Phillips, Nobel lecture: laser cooling and trapping of neutral atoms. *Rev. Mod. Phys.* **70**(3), 721–741 (1998). <https://doi.org/10.1103/RevModPhys.70.721>
29. E. Narevicius, C.G. Parthey, A. Libson, J. Narevicius, I. Chavez, U. Even, M.G. Raizen, An atomic coilgun: using pulsed magnetic fields to slow a supersonic beam. *New J. Phys.* **9**(10), 358 (2007). <https://doi.org/10.1088/1367-2630/9/10/358>
30. E. Narevicius, A. Libson, C.G. Parthey, I. Chavez, J. Narevicius, U. Even, M.G. Raizen, Stopping supersonic beams with a series of pulsed electromagnetic coils: an atomic coilgun. *Phys. Rev. Lett.* **100**(9), 093003 (2008). <https://doi.org/10.1103/PhysRevLett.100.093003>
31. S.Y.T. van de Meerakker, N. Vanhaecke, G. Meijer, Stark deceleration and trapping of OH radicals. *Annu. Rev. Phys. Chem.* **57**(1), 159–190 (2006). <https://doi.org/10.1146/annurev.physchem.55.091602.094337>
32. S.D. Hogan, M. Motsch, F. Merkt, Deceleration of supersonic beams using inhomogeneous electric and magnetic fields. *Phys. Chem. Chem. Phys.* **13**(42), 18705–18723 (2011). <https://doi.org/10.1039/c1cp21733j>
33. H. Ammann, N. Christensen, Delta kick cooling: a new method for cooling atoms. *Phys. Rev. Lett.* **78**(11), 2088–2091 (1997). <https://doi.org/10.1103/PhysRevLett.78.2088>
34. H. Ammann, R. Gray, I. Shvarchuck, N. Christensen, Quantum delta-kicked rotor: experimental observation of decoherence. *Phys. Rev. Lett.* **80**(19), 4111–4115 (1998). <https://doi.org/10.1103/PhysRevLett.80.4111>
35. H. Müntinga et al., Interferometry with Bose-Einstein condensates in microgravity. *Phys. Rev. Lett.* **110**(9), 093602 (2013). <https://doi.org/10.1103/PhysRevLett.110.093602>
36. L. Dupays, D.C. Spierings, A.M. Steinberg, A. del Campo, Delta-kick cooling, time-optimal control of scale-invariant dynamics, and shortcuts to adiabaticity assisted by kicks. *Phys. Rev. Res.* **3**(3), 033261 (2021). <https://doi.org/10.1103/PhysRevResearch.3.033261>
37. M. Kleber, Exact solutions for time-dependent phenomena in quantum mechanics. *Phys. Rep.* **236**(6), 331–393 (1994). [https://doi.org/10.1016/0370-1573\(94\)90029-9](https://doi.org/10.1016/0370-1573(94)90029-9)
38. M. Ben Dahan, E. Peik, J. Reichel, Y. Castin, C. Salomon, Bloch oscillations of atoms in an optical potential. *Phys. Rev. Lett.* **76**, 4508–4511 (1996). <https://doi.org/10.1103/PhysRevLett.76.4508>
39. E. Peik, M. Ben Dahan, I. Bouchoule, Y. Castin, C. Salomon, Bloch oscillations of atoms, adiabatic rapid passage, and monokinetic atomic beams. *Phys. Rev. A* **55**, 2989–3001 (1997). <https://doi.org/10.1103/PhysRevA.55.2989>
40. S.R. Wilkinson, C.F. Bharucha, K.W. Madison, Q. Niu, M.G. Raizen, Observation of atomic Wannier-Stark ladders in an accelerating optical potential. *Phys. Rev. Lett.* **76**, 4512–4515 (1996). <https://doi.org/10.1103/PhysRevLett.76.4512>
41. C.F. Bharucha, K.W. Madison, P.R. Morrow, S.R. Wilkinson, B. Sundaram, M.G. Raizen, Observation of atomic tunneling from an accelerating optical potential. *Phys. Rev. A* **55**, 857–860 (1997). <https://doi.org/10.1103/PhysRevA.55.R857>
42. M.C. Downer, R. Zgadzaj, A. Debus, U. Schramm, M.C. Kaluza, Diagnostics for plasma-based electron accelerators. *Rev. Mod. Phys.* **90**, 035002 (2018). <https://doi.org/10.1103/RevModPhys.90.035002>
43. F. Albert et al., 2020 roadmap on plasma accelerators. *New J. Phys.* **23**(3), 031101 (2021). <https://doi.org/10.1088/1367-2630/abcc62>
44. R.J. England et al., Dielectric laser accelerators. *Rev. Mod. Phys.* **86**, 1337–1389 (2014). <https://doi.org/10.1103/RevModPhys.86.1337>
45. L. Happ, M.A. Efremov, H. Nha, W.P. Schleich, Sufficient condition for a quantum state to be genuinely quantum non-Gaussian. *New J. Phys.* **20**(2), 023046 (2018). <https://doi.org/10.1088/1367-2630/aaac25>
46. C. Kiefer, *Quantum Gravity* (Oxford University Press, Oxford, 2004)

47. G.G. Rozenman, S. Fu, A. Arie, L. Shemer, Quantum mechanical and optical analogies in surface gravity water waves. *Fluids* **4**(2), 96 (2019). <https://doi.org/10.3390/fluids4020096>
48. G.G. Rozenman et al., Projectile motion of surface gravity water wave packets: an analogy to quantum mechanics. *Eur. Phys. J. Spec. Top.* **230**(4), 931–935 (2021). <https://doi.org/10.1140/epjs/s11734-021-00096-y>
49. G.G. Rozenman, M. Zimmermann, M.A. Efremov, W.P. Schleich, L. Shemer, A. Arie, Amplitude and phase of wave packets in a linear potential. *Phys. Rev. Lett.* **122**, 124302 (2019). <https://doi.org/10.1103/PhysRevLett.122.124302>
50. G.G. Rozenman, L. Shemer, A. Arie, Observation of accelerating solitary wavepackets. *Phys. Rev. E* **101**, 050201 (2020). <https://doi.org/10.1103/PhysRevE.101.050201>
51. G.G. Rozenman, W.P. Schleich, L. Shemer, A. Arie, Periodic wave trains in nonlinear media: Talbot revivals, Akhmediev breathers, and asymmetry breaking. *Phys. Rev. Lett.* **128**, 214101 (2022). <https://doi.org/10.1103/PhysRevLett.128.214101>
52. G.G. Rozenman, D.I. Bondar, L. Shemer, W.P. Schleich, A. Arie, Observation of Bohm trajectories and quantum potentials (to be published)
53. G.G. Rozenman, F. Ullinger, M. Zimmermann, M.A. Efremov, W.P. Schleich, L. Shemer, A. Arie, Observation of 'black hole' singularities with freely propagating waves (to be published)
54. F. Ullinger, M. Zimmermann, W.P. Schleich, The logarithmic phase singularity in the inverted harmonic oscillator. *AVS Quantum Sci.* **4**(2), 024402 (2022). <https://doi.org/10.1116/5.0074429>
55. M.O. Scully, S. Fulling, D.M. Lee, D.N. Page, W.P. Schleich, A.A. Svidzinsky, Quantum optics approach to radiation from atoms falling into a black hole. *Proc. Natl. Acad. Sci.* **115**(32), 8131–8136 (2018). <https://doi.org/10.1073/pnas.1807703115>
56. G.G. Rozenman, F. Ullinger, M. Zimmermann, M.A. Efremov, W.P. Schleich, L. Shemer, A. Arie, Emulating black holes using surface gravity water waves, Snowbird Utah (2022)
57. G.G. Rozenman, et al., Phase space dynamics of wave packets in the inverted harmonic oscillator (to be published)
58. D. Becker et al., Space-borne Bose-Einstein condensation for precision interferometry. *Nature* **562**, 391–395 (2018). <https://doi.org/10.1038/s41586-018-0605-1>
59. D.C. Aveline et al., Observation of Bose-Einstein condensates in an Earth-orbiting research lab. *Nature* **582**(7811), 193–197 (2020). <https://doi.org/10.1038/s41586-020-2346-1>

Publisher's Note Springer Nature remains neutral with regard to jurisdictional claims in published maps and institutional affiliations.

Authors and Affiliations

Harald Losert¹  · Freyja Ullinger^{1,2}  · Matthias Zimmermann²  · Maxim A. Efremov^{1,2}  · Ernst M. Rasel³ · Wolfgang P. Schleich^{1,4}

✉ Harald Losert
harald.losert@alumni.uni-ulm.de

¹ Institut für Quantenphysik and Center for Integrated Quantum Science and Technology (IQST), Universität Ulm, 89081 Ulm, Germany

² German Aerospace Center, Institute of Quantum Technologies, 89081 Ulm, Germany

³ Institut für Quantenoptik, Gottfried Wilhelm Leibniz Universität Hannover, 30167 Hannover, Germany

⁴ Hagler Institute for Advanced Study at Texas A&M University, Texas A&M AgriLife Research, Institute for Quantum Science and Engineering (IQSE), and Department of Physics and Astronomy, Texas A&M University, College Station, TX 77843-4242, USA